CARPE DIEM
CENTRE FOR WATER RESOURCES RESEARCH
DELIVERABLE 9.3
FLOOD ESTIMATING AND FORECASTING USING SIMPLE LUMPED CATCHMENT MODELS IN THE DARGLE CATCHMENT

by
Micheal Bruen, Benoit Parmentier

December 2004
Department of Civil Engineering
University College Dublin

Table of Contents

List of Tables

List of Figures

Chapter 1

Introduction to lumped model comparison

An important part of this section of the Carpe Diem project is to assess the validity of radar rainfall estimates for hydrological analysis and flood forecasting. In the Centre for Water Resources Research two very different types of model, each with a very different approach to the spatial aspects, were implemented and compared; lumped models and a distributed model. This report describes the lumped models and their implementation. A separate report (Deliverable) describes the distributed model and another compares the performance of all the models. Two types of lumped model are tested;

- the Unit-Hydrograph (black box model type),
- the SMARG (conceptual model type.

Chapter 2

Overview of the unit-hydrograph approach

2.1 Definition and Assumptions

The T-period Unit-Hydrograph (UH) of a catchment can be defined as the hydrograph of direct runoff resulting from a fixed given pattern and unit volume of effective rainfall, occurring over that catchment at a constant rate during a period of time of duration T. It has been first described by Sherman (1932). In this thesis, the term "direct runoff" is taken to mean the total discharge at the catchment outlet minus the baseflow, i.e. the fast component of total runoff at the basin outlet.

The essential assumption of unit hydrograph theory is that the relationship between rainfall excess and surface runoff is the one of a linear time invariant system. One of the best classical discussions of unit hydrograph procedures is that given in "Element of Applied Hydrology" by Johnstone and Cross (1949):

"The three basic propositions of unit hydrograph theory, all of which refer solely to the surface-runoff hydrograph are:

1. For a given drainage basin, the duration of surface runoff is essentially constant for all uniform intensity storms of the same length, regardless of differences in the total volume of the surface runoff.

2. For a given drainage basin, if two uniform intensity storms of the same length produce

different total volumes of surface runoff, then the rates of surfaces runoff at corresponding time t, after the beginning of the two storms, are in the same proportion to each other as the total volumes of the surface runoff.

3. The time distribution of surface runoff from a given storm period is independent of concurrent runoff from antecedent storm periods."

The principle of proportionality is expressed in propositions 1 and 2. The principle of superposition is contained in proposition 3. Linear time-invariant systems show the superposition property.

It is recognised that the non-linearity of the whole catchment runoff process is mainly contained in the separation of total rainfall into effective rainfall (Duband et al., 1993) and also in the baseflow separation , so that the catchment behavior in relation to direct runoff and excess rainfall may be assumed linear. Dooge (1973) recalls that although the assumptions of linearity and time invariance for a catchment system are not strictly correct, we are content to adopt them as long as they are useful. Linear methods are relatively simple, well developed and acceptable for engineering purposes.

2.2 Mathematical representation

We can express the relationship between the effective rainfall (input x) and the direct runoff (output y) by the convolution integral:

$$y(t) = \int_0^t h(\tau)x(t-\tau)d\tau \tag{2.1}$$

where, $h(\tau)$ is the transfer function characterizing the impulse response of the system, also called the instantaneous unit hydrograph (Dooge, 1973).

In practice, data are rarely analyzed in continuous form. A discrete formulation of the convolution integral is:

$$y(sT) = \sum_{k=0}^{k=s} h(kT)x\big((s-k)T\big) \tag{2.2}$$

where, $x(sT)$ is the volume of effective rainfall during the interval $t= sT$ to $t= (s+1)T$ and $y(sT)$ is the value of the direct runoff sampled at time $t= sT$. $h(sT)$ represents the T period unit hydrograph, i.e. the direct runoff due to unit volume of effective rainfall during

an initial interval of duration T. This equation applies to isolated events. Eagleson et al. (1966) has shown that the convolution relation also holds between the auto-correlation of the input series and the cross-correlation of the input with the output series.

If there are p output values, the discrete convolution equation gives p simultaneous linear algebraic equations, which can, for convenience, be written in matrix form as:

$$\mathbf{Xh} = \mathbf{y} \tag{2.3}$$

where:

- $\mathbf{X}$ is a p x n matrix formed from the m input series values,
- $\mathbf{y}$ is a vector containing the p output series values,
- $\mathbf{h}$ is a vector representing the, as yet unknown, n values of the pulse response.

Equation (2.4) shows the matrix and the vectors contents for Equation (2.3) for the case $m < n$ and for an isolated event:

$$\begin{bmatrix}
x_1 & 0 & 0 & \cdots & 0 & 0 & 0 \\
x_2 & x_1 & 0 & \cdots & 0 & 0 & 0 \\
x_3 & x_2 & x_1 & \cdots & 0 & 0 & 0 \\
\cdot & \cdot & \cdot & \cdots & \cdot & \cdot & \cdot \\
\cdot & \cdot & \cdot & \cdots & \cdot & \cdot & \cdot \\
x_m & x_{m-1} & x_{m-2} & \cdots & \cdot & \cdot & \cdot \\
0 & x_m & x_{m-1} & \cdots & \cdot & \cdot & \cdot \\
0 & 0 & x_m & \cdots & \cdot & \cdot & \cdot \\
\cdot & \cdot & \cdot & \cdots & \cdot & \cdot & \cdot \\
\cdot & \cdot & \cdot & \cdots & \cdot & \cdot & \cdot \\
0 & 0 & 0 & \cdots & x_1 & 0 & 0 \\
0 & 0 & 0 & \cdots & x_2 & x_1 & 0 \\
0 & 0 & 0 & \cdots & x_3 & x_2 & x_1 \\
\cdot & \cdot & \cdot & \cdots & \cdot & \cdot & \cdot \\
\cdot & \cdot & \cdot & \cdots & \cdot & \cdot & \cdot \\
0 & 0 & 0 & \cdots & x_m & x_{m-1} & x_{m-2} \\
0 & 0 & 0 & \cdots & 0 & x_m & x_{m-1} \\
0 & 0 & 0 & \cdots & 0 & 0 & x_m
\end{bmatrix}
\begin{bmatrix}
h_1 \\ h_2 \\ h_3 \\ \cdot \\ \cdot \\ h_m \\ h_{m+1} \\ h_{m+2} \\ \cdot \\ \cdot \\ h_{n-2} \\ h_{n-1} \\ h_n
\end{bmatrix}
=
\begin{bmatrix}
y_1 \\ y_2 \\ y_3 \\ \cdot \\ \cdot \\ y_m \\ y_{m+1} \\ y_{m+2} \\ \cdot \\ \cdot \\ y_{n-2} \\ y_{n-1} \\ y_n \\ \cdot \\ \cdot \\ y_{p-2} \\ y_{p-1} \\ y_p
\end{bmatrix} \tag{2.4}$$

The matrix $\mathbf{X}$ has a particular structure. The number of columns is always less than the number of rows and often considerably less. In ideal conditions:

$$p = m + n - 1 \tag{2.5}$$

In practice, because of data errors and uncertainty, it may be difficult to estimate the length of the output series.

The standard estimation problem is to determine the values of the pulse response ordinates, $\mathbf{h}$, from measurements of the input series, $\mathbf{x}$, and the output series, $\mathbf{y}$.

2.3 Limitation of the Unit-Hydrograph

Catchments are inherently non-linear in their response to rainfall, so that the linearity assumption is always an approximation. It sometimes gives good results, but there are catchments for which it is not appropriate.

A key assumption for the transfer of a derived unit-hydrograph to another storm is the time invariance of the spatial distribution of the rainfall, the reference being the particular event used to derive that unit-hydrograph. Being a highly spatially variable process by nature, precipitation and hence effective rainfall will rarely occur uniformly over a catchment. That non-uniform spatial distribution of the precipitation process will often change from one storm event to another one. However, the error due to the change in rainfall distribution over a larger catchment can be minimized by defining sub-catchments and deriving unit-hydrographs for each of them, assuming again that the precipitation distribution is preserved in time over those sub-catchments.

Furthermore, the catchment's response to an individual rainstorm depends strongly on the initial state of the catchment, and particularly to its soil moisture content and hence the validity of the time-invariance assumption may be questionable.

2.4 Use of the Unit-Hydrograph

Despite all its limitations described above, the unit-hydrograph method is usually accepted as a practical and useful tool, since its theory is simple to be understood and its hypothesis

is particularly adequate in the range of floods experienced on natural basins (Singh, 1988). Among these uses:

- it can be used to determine the catchment response due to intense rainfall events, e.g. for flood forecasting and warning.
- it can also help in the assessment of the effect of flood protection works on basin response by comparing unit-hydrographs before and after completion of the works.

2.5 Methods of Identification

Hydrologists have encountered practical difficulties in deriving realistic unit-hydrographs and have developed a number of useful practical methods, (Dooge and Bruen, 1989). An important step towards the identification of the unit-hydrograph itself is the derivation of both the direct runoff and the effective rainfall. The nature of the loss function and of the baseflow separation method do have an influence in the characteristics of the identified unit-hydrograph. In most identification methods presented in the following list, the loss function and baseflow separation method are arbitrary.

- Collins (1939) suggested a variation of the trial and error approach in which the most recent estimate of the unit-hydrograph is applied to all rainfall values except the maximum one. The resulting computed runoff is subtracted from the actual runoff to give the runoff due to the maximum ordinate alone and this is used to update the previous estimate of the unit-hydrograph. Collins' method is equivalent to selecting and solving the n equations which contain the maximum rainfall value and neglecting the other equations.
- Barnes (1959) suggested using both backward and forward substitutions and the adjustment of the input value until the estimates from each method are close.
- Least-squares methods allow all p equations to be used simultaneously in determining a solution which is optimal in the "minimum squares deviations" sense (Snyder, 1955). The unit-hydrograph is the solution of:

$$\left(\mathbf{X}^T\mathbf{X}\right)\mathbf{h} = \mathbf{X}^T\,\mathbf{y} \tag{2.6}$$

- Kuchment (1967) applied the regularization technique developed by Ivanov (1963) to derive a smoothed least-squares estimate of the unit-hydrograph. A description of the ridge regression technique, also called damped or smoothed least-squares, may be found in Weisberg (1980) and in Draper and Smith (1998). This extension of the least-squares method can be implemented with a minimal amount of extra computations (Bruen and Dooge, 1984). Here, the unit-hydrograph is the solution of:

$$\left(\mathbf{X}^T\mathbf{X} + \gamma\,\mathbf{I}\right)\mathbf{h} = \mathbf{X}^T\,\mathbf{y} \tag{2.7}$$

  where $\mathbf{I}$ is the identity matrix amd γ the smoothing parameter.

- O'Donnell (1960) applied linear transform methods to unit-hydrograph estimation and used the simple linkage equation between the harmonic transform of the input, output and unit-hydrograph. Dooge (1965) used Laguerre transforms and (Dooge and Garvey, 1978) used Meixner transforms, both of which have more complex linkage equations, to estimate unit-hydrographs but are more suited to heavily damped systems, such as catchments.

- Gouy (1991) developed a method of identification mixing ARMAX time-series models and polynomial divisions, requiring rainfall and flow information.

- Duband et al. (1993) suggested a more complex iterative-alternative method called FDTF (for First Derivative Transfer Function). It is free from the arbitrary selection of a loss function to derive the effective rainfall and of a method used to derive the direct runoff.

- Other methods using z-transforms and independent of rainfall data: the De Laine method, the Turner method and the root separation method.

2.6 Effects of Data Errors

Almost all the direct algebraic methods used in practice reduce the problem to solving a square set of linear equations:

$$\mathbf{A}\,\hat{\mathbf{h}} = \mathbf{b} \tag{2.8}$$

where, the reduction of matrix $\mathbf{X}$ and vector $\mathbf{y}$ in Equation (2.3) to the matrix $\mathbf{A}$ and to the vector $\mathbf{b}$ respectively depends only on the estimation method.

For the direct methods, such as forward-backward substitution or the Collins method, the matrix $\mathbf{A}$ contains a selection of rows from the convolution matrix $\mathbf{X}$. The vector $\mathbf{b}$ contains the corresponding values from the output series $\mathbf{y}$.

For the case of the least squares methods (refer to Equation (2.6)):

$$\mathbf{A} = \mathbf{X}^T \mathbf{X} \tag{2.9}$$

$$\mathbf{b} = \mathbf{X}^T \mathbf{y} \tag{2.9'}$$

For the smoothed least squares method, a constant γ is added to the diagonal of the matrix $\mathbf{X}^T\mathbf{X}$ (Draper and Smith, 1998; Weisberg, 1980):

$$\mathbf{A} = \mathbf{X}^T\mathbf{X} + \gamma\,\mathbf{I} \tag{2.10}$$

where, $\mathbf{I}$ is the identity matrix.

For all these methods, the unit-hydrograph estimate is the solution of Equation (2.8), which can be written formally as:

$$\hat{\mathbf{h}} = \mathbf{A}^{-1}\,\mathbf{b} \tag{2.11}$$

The presence of the inverse of a matrix in the formal solution raises the question of numerical stability of an estimate based on data which are subject to measurement errors. A convolution of the effective rainfall and the unit-hydrograph is a smoothing procedure. Conversely, a deconvolution to estimate the unit-hydrograph from effective rainfall and direct-runoff amplifies any data or modelling errors. This amplification often leads to unstable and physically unrealistic unit-hydrograph estimates with the earlier methods of solution (Dooge and Bruen, 1978, 1989).

Standard relationships from linear algebra theory may then be used to analyze the amplification: a unique real valued function of the matrix $\mathbf{A}$, called its condition number, is found to provide an upper bound of the error amplification (Forsythe and Moler, 1967; Lawson and Hanson, 1974).

The condition number is given as:

$$C(\mathbf{A}) = \left|\frac{\lambda_{max}}{\lambda_{min}}\right|^{1/2} \tag{2.12}$$

where λ_{max} and λ_{min} are the largest and the smallest eigenvalues of the matrix $\mathbf{A}$ respectively.

We hereinafter illustrate the behaviour of the condition number for a very simple case where only two unit-hydrograph ordinates have to be estimated and for which a closed form result may be obtained, as investigated by Dooge and Bruen (1989).

In the case of two unknown unit-hydrograph ordinates, the matrix $\mathbf{A}$ has only two rows and two columns. It can hence be written as:

$$\mathbf{A}^T\,\mathbf{A} = \begin{bmatrix} c_{11} & c_{12} \\ c_{21} & c_{22} \end{bmatrix} \tag{2.13}$$

The eigenvalues λ of the matrix are the roots of the equation:

$$(c_{11} - \lambda)\,(c_{22} - \lambda) - c_{12}c_{21} = 0 \tag{2.14}$$

And in this case the condition number is:

$$C(\mathbf{A}) = c + \sqrt{c^2 - 1} \tag{2.15}$$

where:

$$c = \frac{c_{11} + c_{22}}{2\,\sqrt{c_{11}c_{22} - c_{12}c_{21}}} \tag{2.16}$$

For high values of c, the condition number increases almost linearly with c, which is inversely proportional to the square-root of the determinant of the matrix $\mathbf{A}^T\mathbf{A}$.

For the ordinary-least squares method, in the case of two unknown unit-hydrograph ordinates, the spectral condition number can be written as:

$$C(\mathbf{A_{LS}}) = \frac{\phi_0 + \phi_1}{\phi_0 - \phi_1} \tag{2.17}$$

where $\phi_0 = \sum_{i=1}^{i=m} x_i^2$ and $\phi_1 = \sum_{i=1}^{i=m-1} x_i x_{i+1}$,

the x_i being the input series (effective rainfall) and:

$$\mathbf{A} = \mathbf{X}^T\mathbf{X} = \begin{bmatrix} \phi_0 & \phi_1 \\ \phi_1 & \phi_0 \end{bmatrix} \tag{2.18}$$

The condition number does not have an upper bound, and is an increasing function of the length of the input series and its lag-one auto-correlation.

For the smoothed-least squares method, in the case of two unknown unit-hydrograph ordinates, the condition number is:

$$C\big(\mathbf{X}^T\mathbf{X} + \gamma\,\mathbf{I}\big) = \frac{\phi_0 + \phi_1 + \gamma}{\phi_0 - \phi_1 + \gamma} \tag{2.19}$$

Thus, for any positive value of γ, the condition number is lower for the smoothed-least squares than for the ordinary least-squares solution. As the value of γ increases, the condition number for the estimation decreases and the estimate of the unit-hydrograph becomes more stable. It is also an increasing function of the length of the input series and its lag-one auto-correlation.

The condition number offers no information about the bias in estimating $\mathbf{h}$. However it is related to the numerical stability of the method. For instance, for the forward substitution method, the condition number indicates that error amplification is greater when the intensity of the effective rainfall increases with time during a storm, rather than decreases. The better performance of Collins' method for most inputs can be explained in terms of the condition number.

In order to compare the two least squares methods of identification (ordinary and smoothed), we can also analyze the value of the expected value of the sum of squares of the errors in the estimate, noted E_S.

The ordinary least-squares estimate, $\hat{\mathbf{h}}_{OLS}$, is not biased and E_S can be written as:

$$E_S = E\Big\{ \big(\hat{\mathbf{h}}_{OLS} - \mathbf{h}\big)^T \big(\hat{\mathbf{h}}_{OLS} - \mathbf{h}\big) \Big\} = \sigma^2 \,\mathrm{trace}\big(\mathbf{X}^T\mathbf{X}\big) = \sigma^2 \sum_{i=1}^{i=n} \frac{1}{\lambda_i} \tag{2.20}$$

where, the λ_i are the eigenvalues of the matrix $\mathbf{X}^T\mathbf{X}$ and σ^2 is the output data error variance. It can be shown that the sum of the inverse of the eigenvalues is minimal when the input series has only one non-zero value (short series and zero auto-correlation).

For the smoothed-least squares, the estimate of $\mathbf{h}$ is biased, and E_{SSes} can be written as:

$$E_S = S\big(\mathrm{bias}\big(\hat{\mathbf{h}}\big)\big) + \sigma^2 \sum_{i=1}^{i=n} \frac{1}{\lambda_i + \gamma} \tag{2.21}$$

where $S(\mathrm{bias}(\hat{\mathbf{h}}))$ is the sum of squares of the bias of the estimator and increases as γ increases. However, the second term decreases as γ increases and it can be shown (Hoerl and Kennard, 1970) that there is a positive value of γ for which the sum of the two terms is a minimum, i.e. an optimal compromise between the bias on the estimate and the stability of the method.

Chapter 3

The SMAR model

Conceptual, quasi-physical, models attempt to simulate the major hydrological processes involved in the transformation mechanism of the input (rainfall and/or evaporation) into the output (runoff or discharge). Use of empirical relations and/or simplified assumptions are made to avoid excessive mathematical complexities in describing the various sub-processes, some of which are yet to be understood in their real form and also to avoid the need to procure large sets of varied information which may be required by ideal mathematical representations. Usually, parameters are part of the representation of the physical processes considered in the structure of a conceptual model. In reality, such models often incorporate only simplified approximations to the physical processes involved, whence the qualifier "quasi-physical".

The SMAR model was developed in Galway University. It is now a component of the GFMFS (Galway Flow Modeling and Forecasting System). A visual interface has been developed and the model has been widely used for flow simulation and forecasting (O'Connor et al., 2001; Tan and O'Connor, 1996; Tan et al., 1996; Zhang, 1992; Zhang et al., 1994). The following description is based on the Galway Flow Modelling and Forecasting System (GFMFS) user's manual.

The SMAR model is a simple lumped conceptual rainfall-evaporation-runoff model. It is designed to incorporate an approximate representation of some of those physical processes known to have an important role in the generation of stream flow by a number of interconnected conceptual storage sub-systems. SMAR is an abbreviation of the Soil Moisture Accounting and Routing procedure (Kachroo, 1992). This model was originally known as

the layers model (O'Connell et al., 1970), its water-balance component being based on the "Layers Water Balance Model" proposed in 1969 by Nash and Sutcliffe (Clarke, 1994). In the GFMFS, a modified version of the SMAR layers model, called SMARG version, due to both Khan (1986) and Liang (1992), is used. For use in karstic type of catchments where a significant quantity of generated runoff is lost to underground channels or sinkholes and does not appear at the catchment outlet, a version called SMARK incorporating a modification of the ground water flow is also included. It differs from its nine-parameter parent SMAR model in one fundamental respect to the extent that it incorporates an additional parameter F to abstract a loss component from any excess runoff. This loss component is interpreted as a separate outflow function L from the catchment system, defining that part of the rainfall that does not evaporate and yet will never subsequently contribute to the discharge at the outflow gauging station.

In the structure of the SMAR model (Figure 3.1), two distinct complementary components can be identified. The first is a non-linear water balance (soil moisture accounting procedure) component that keeps account of the balance between the rainfall, the evaporation, the runoff and the simulated soil storage using a number of empirical and assumed functions which are, however, physically realistic or at least physically plausible. The second is a routing component which simulates the attenuation and the diffusive effects of the catchment by routing the different generated runoff components, through linear time invariant storage systems.

The essence of the SMAR model is the concept of soil layers. The catchment is visualised as being composed of a set of horizontal soil layers, each of which may contain water up to a maximum depth of 25 mm except for the bottom layer which may have a maximum depth less than 25 mm. The total combined water storage depth of these layers is a parameter of the model (Z). Default maximum value of Z is kept at 125 mm.

The evaporation input (E) to the model is either the Pan evaporation depth or that obtained from Penman's equation, which when multiplied by a parameter T (less than unity), is converted to an estimate of the potential evaporation depth over the catchment.

Evaporation only occurs from the layers when there is no rainfall or when the rainfall is not sufficient to satisfy the potential evaporation demand ($T \times E$). Any evaporation

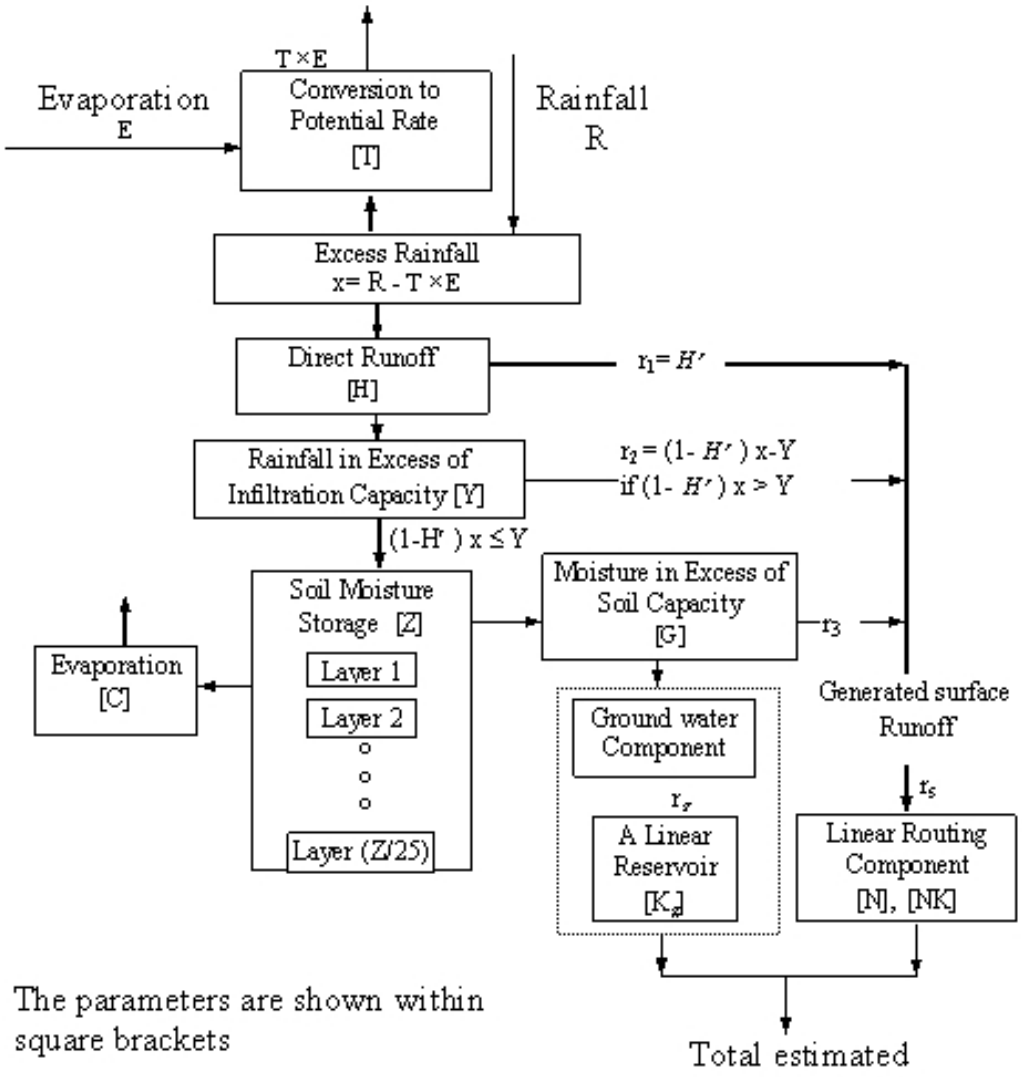

Figure 3.1: SMARG model structure

from the first layer occurs at the potential rate. On the depletion of the water depth in the first layer, any evaporation from the second layer occurs at the potential rate multiplied by a parameter C ($C \leq 1$). On the depletion of the water depth of the second layer, any subsequent evaporation from the third layer occurs at rate of C^2 and so on. Hence, if the all layers were full and there was no subsequent rainfall, then a constant potential evaporation applied to the catchment would reduce the soil moisture storage in, approximately, an exponential manner. Such evaporation would continue until either the storage of all the layers was depleted or the potential evaporation demand was fully satisfied.

In rainy days, provided the rainfall exceeds the potential evaporation ($T \times E$) depth, runoff takes place. A fraction H' of the excess rainfall, i.e. the rainfall less than the potential

evaporation, contributes to the generated runoff by producing the direct generated runoff component r_1. H' is considered to be directly proportional to the ratio of the available water depth to the maximum depth in the top five layers, or in the total set of layers if the number of the layers is less than five i.e.

$$H' = H \frac{W}{W_{max}} \tag{3.1}$$

The constant of proportionality H is a parameter of the model, with H' having a value between zero and H.

Allowing the direct generated runoff to vary as a function of the available water in the top five layers (or if $Z < 125mm$ in the whole stack of layers) is a modification due to Khan (1986), of the original version of the SMAR model presented by O'Connell et al. (1970) in which the direct generated runoff occurs without any consideration of the available soil moisture depth in the layers.

Any remainder of the excess rainfall, after the subtraction of r_1, which exceeds the maximum infiltration capacity Y (in mm/day), also contributes to the generated runoff as r_2, the component of runoff in excess of the infiltration capacity. The remaining rainfall, after subtraction of both the direct runoff r_1 and the runoff in excess of infiltration capacity r_2 (if any), replenishes each soil layer in turn beginning from the first (i.e. the top) layer downwards, until either the rainfall is exhausted or all layers are full. Any still remaining surplus is further divided into two portions, the first portion being envisaged as a groundwater runoff component r_g while the second is considered as a subsurface runoff component r_3. This r_3 component is added to the direct runoff r_1 and to that in excess of infiltration capacity r_2 to produce the total generated surface runoff r_s as $r_s = r_1 + r_2 + r_3$. The division into two parts of the final surplus emanating from the layers is controlled by a weight parameter G. This division was introduced by Liang (1992) as a further refinement to Khan (1986) version of the SMAR model in which the whole surplus is directly added to other generated surface runoff components to give a single composite generated runoff.

The total generated surface runoff (i.e. $r_s = r_1 + r_2 + r_3$) is routed through a two parameter distribution function. In the GFMFS, three two-parameter distribution options are available for routing the generated "surface runoff" component of the SMAR model,

namely, the classic gamma distribution (Nash-cascade) model (Nash, 1958) having the shape parameter N and the lag NK, its discrete counterpart the Negative Binomial distribution (O'Connor, 1976) having parameters N (number of linear reservoirs in the cascade) and K (storage coefficient of each linear reservoir), and the sharp-peaked Inverse Gaussian distribution (Bardsley, 1983) for flashy catchments having parameters j and m.

The groundwater runoff component r_g is routed through a single linear reservoir with a storage coefficient parameter K_g.

The sum of the outputs of these two routing components is the SMAR model estimated outflow.

The surface runoff component of the original SMAR model is routed through a Nash-cascade of N equal linear reservoirs, each having the storage coefficient NK. For optimisation, the parameters n and the product NK, instead of N and K, are chosen so that the optimised value of NK, which is the mean of the impulse response function in the above equation, indicates the time lag between the pulsed input and the corresponding output.

The generated ground water series r_g from the water balance component is routed through a single linear reservoir having storage coefficient K_g.

From the conceptual modelling point of view, the initial ground water condition is generally unknown and an initial value of zero ground water flow is assumed for use in both model forms. Apart from this, it is also assumed that all the soil moisture-holding layers are initially full to their capacity values. The warm up period may be considered as very short.

Thus the SMARG version of the SMAR model has nine parameters, five of which control the overall operation of the water-budget component, while the remaining four parameters (including a weighting parameter which determines the amount of generated "groundwater runoff") control the operation of the routing component. Some of the parameters may be fixed at appropriately chosen values while the values of the rest are usually estimated empirically by optimisation to minimise the selected measure of error between the observed and the model estimated discharges. The parameters of the SMARG model are shown in the Table 3.1 below.

The SMARG model requires a set of data series for precipitation and evapotranspiration

Parameter	Description
Z	The combined water storage depth capacity of the layers (mm)
T	A parameter (≤ 1) that converts the given evaporation series to the model-estimated potential evaporation series
C	The evaporation decay parameter, facilitating lower evaporation rates from the deeper soil moisture storage layers
H	The generated "direct runoff" coefficient
Y	The maximum infiltration capacity depth (mm)
N	The shape parameter of the Nash gamma function "surface runoff" routing element; a routing parameter
NK	The scale (lag) parameter of the Nash gamma function "surface runoff" routing element; a routing parameter
G	The weighting parameter, determining the amount of generated "groundwater" used as input to the "groundwater" routing element
K_g	The storage coefficient of the "groundwater" (linear reservoir) routing element; a routing parameter

Table 3.1: Parameters of the SMARG model (9).

for simulation, and an additional data series for calibration. The model may run at hourly or daily time step.

The calibration of the model may be carried out by direct measurement of the parameters, by trial and error, by automatic calibration or by a combination of those methods. An automatic calibration with constraints on the parameters is preferred in this study.

Chapter 4

THE DARGLE CATCHMENT

4.1 General

The Dargle is a short river of approximately 15 km length, which, together with a number of tributaries, drains a 122 km^2 catchment on the eastern side of the Dublin Mountains. It flows into the Irish Sea through the large town of Bray. Although small, the catchment has great variety. Its elevation varies from close to sea level to over 700 m above sea level, Figure 4.1. Land use comprises urban areas in the lower coastal areas of the catchment, tillage, pasture/sheep farming, forestry and peaty scrubland in the headwater areas. In particular, the catchment can be divided into twelve sub-catchments, each with one of these land-uses predominant, as seen on Table 4.1. This makes it a good catchment for comparative studies of the effects of land use. Because it flows into the sea at a scenic location near a number of beaches there is concern that it may affect bathing water quality, especially just after floods.

Annual rainfall amounts varies with altitude and increases from less than 1000 mm at the coast to over 2000 mm on the peaks towards the western side of the catchment. The Dargle is subject to flash floods that can have peaks of well over $100m^3/s$. It has predominantly a gravel or rocky bed. Twelve (12) electronic recording water level recorders have been installed at the outlets of most of the sub-catchments and 4 tilting bucket recording rain gauges within the catchment (see Figure 4.2). One rain gauge is at sea level, one at above 350 m altitude and the remaining two at intermediate altitudes.

Rating curves have been established and are being updated for the water level recorders,

by current meter flow gauging, ultrasonic flow measurement and hydraulic computer simulation.

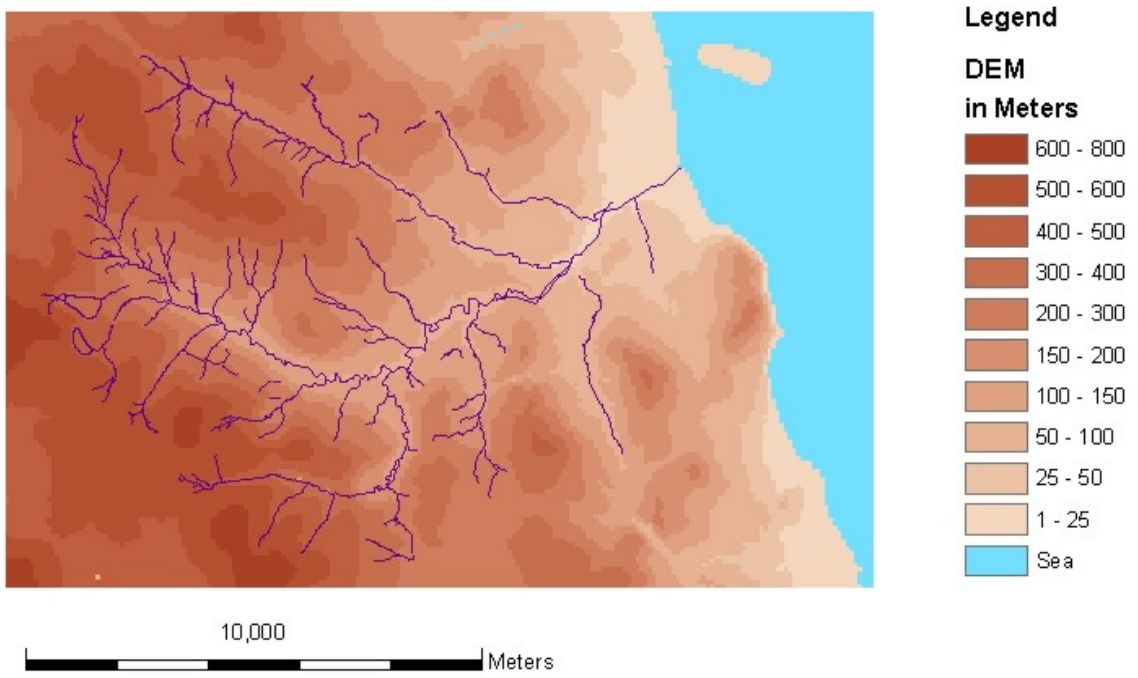

Figure 4.1: Digital elevation model of the Dargle catchment

4.2 Rainfall data

Three RainLog tipping-bucket automatic recording rain gauges were installed within the rural part of the catchment, (i) near Djouce Wood, (ii) in Powerscourt Demesne and (iii) at the Stone Quarry in Glencullen valley. A fourth one was installed at the sewage pumping station in Bray (see Figure 4.2). These have a resolution (bucket capacity) of 0.2 mm and record the time (to within a minute) and date of every bucket tip. The sites were chosen to give a distribution covering a range of altitudes, and both north-south and east-west axes within the catchment to establish any spatial variation in the overall rainfall pattern. FORTRAN programs were written to extract rainfall time series for any specified time-interval, e.g. daily, hourly, minutely, etc, from the recorded data. As expected, there is considerable variation in rainfall amounts with altitude, decreasing from west to east. The totals recorded during the period 22 July 2000 to 13 Nov 2000 were Djouce (618 mm), Stone Quarry (534 mm) and Powerscourt Demesne (515 mm). The correlation of daily rainfall

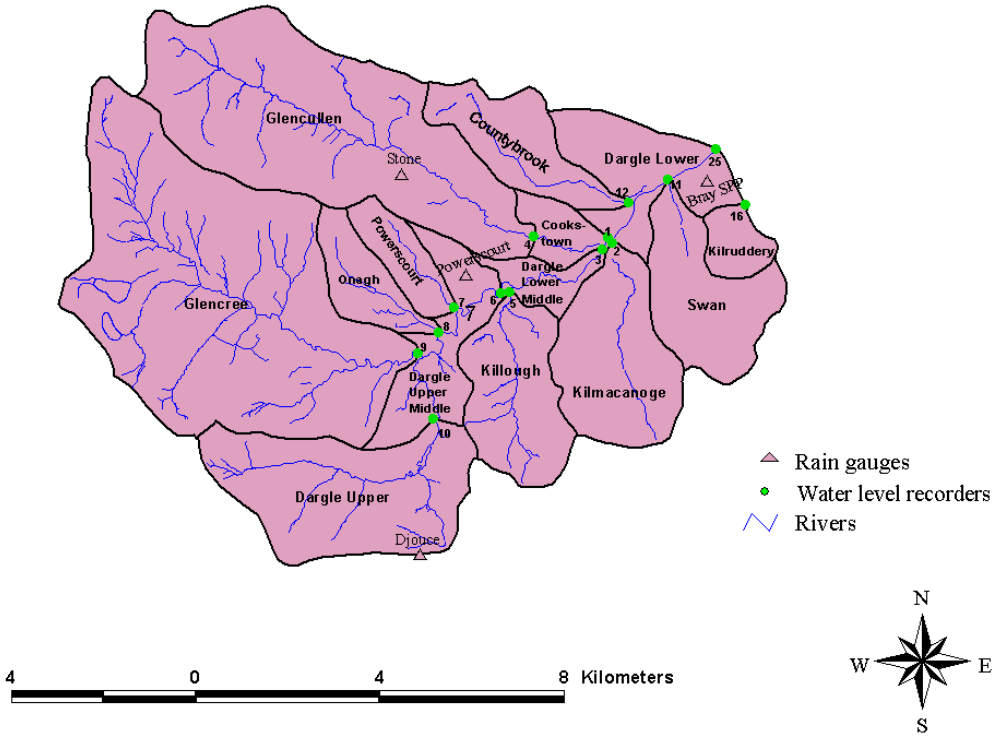

Figure 4.2: Locations of instruments in the Dargle catchment (level recorders locations similar to biological quality points; points 16 and 25 only used for water quality sampling)

totals between Stone Quarry (Glencullen valley) and Powerscourt Demesne (Dargle valley) was quite close (Figure 4.3). The correlation between the higher Djouce values and the others was still good but with more scatter for the higher rainfall amounts (Figure 4.4).

4.3 Water levels and flows

Eleven OTT Thalimedes and one OTT Opthalimedes bubble automatic recording water level recorders were installed in the catchment. In all, 12 different sites are used: see Table 3 and Figure 4. All instruments recorded water levels to a precision of 1 mm and, for the period of study, were set to record the water level every five minutes.

The sites were chosen with a number of objectives in mind. They had to be secure and safely accessible at all times, day or night, during high flows. They also had to offer a

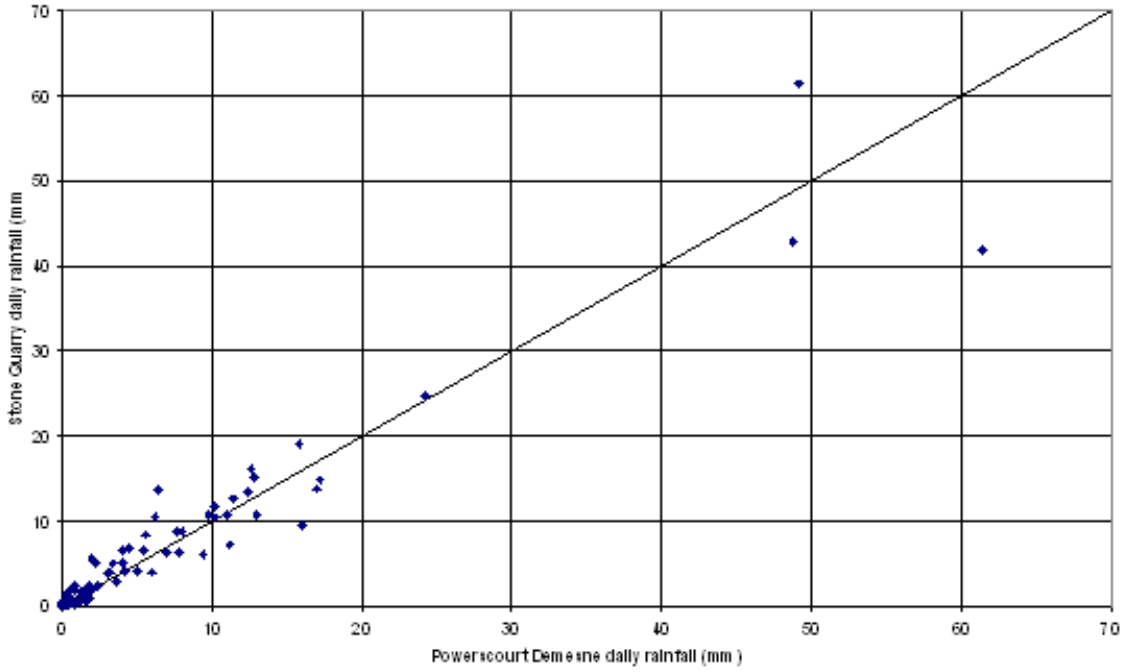

Figure 4.3: Correlation of daily rainfall amounts in middle Dargle catchment (Powerscourt) with middle Glencullen catchment (Stone Quarry).

reasonable prospect of establishing a rating relationship between water levels and flows, especially high ones. The sites chosen reflect a balance between these objectives. Accessibility and safety requirements often dictated the choice of sites near existing bridges. Accurate measurement of low flows was not a priority and was not feasible within the parameters of this project as it requires the construction of control structures in the channels.

The establishment of rating curves takes many years and requires spot gauging at a wide range of different flows. Such work has begun during this project and will be continued by UCD. For the purposes of this project, preliminary rating relationships were established by surveying the channel in the vicinity of the gauge and for some distance downstream and using a steady-flow computer program (HECRAS) to simulate water levels for different discharges through the reach. This establishes first estimates of a rating relationship which can be refined as more spot-flow measurements are taken with a current meter for medium-range flows and an ultrasonic time-of-travel device for high flows. The spot-flow measurements taken as part of this study were used to help calibrate the rating relationships. The preliminary rating curves are very sensitive to the choice of Manning's coefficient for the reaches and of the downstream boundary conditions. A number of the gauging sites

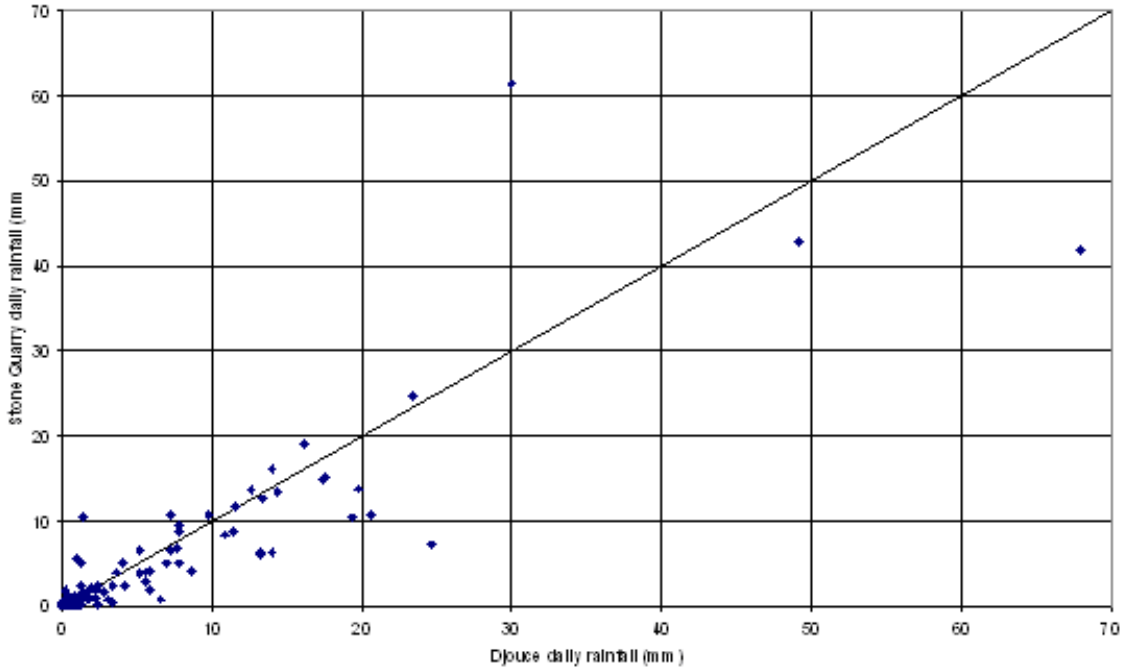

Figure 4.4: Correlation of daily rainfall amounts in high Dargle catchment (Djouce) with middle Glencullen catchment (Stone Quarry).

offered a reasonable expectation of producing critical flow conditions a short distance downstream of the site during high flows, while "uniform" flow sections were assumed at other sites. The gauge on the Kilmacanogue site is just upstream of a culvert entrance that is expected to offer an inlet control during high flows.

Subcatchment	percentage of area under land use						Area (km^2)
	Arable	Built-up	Forest	Lake & Rock	Pasture	non-agric veg.	
Waterfall - North	0.00	0.67	29.70	0.00	7.16	62.47	12.95
Onagh (Glencree)	0.07	0.78	29.50	1.23	12.94	55.48	33.87
Onagh Stream	4.92	3.28	33.34	3.99	45.54	8.92	3.34
Powerscourt Stream	24.91	5.49	38.18	0.06	28.77	2.60	2.69
Tinnahinch Bridge	2.41	2.19	30.62	0.94	16.79	47.04	52.85
Killough Bridge	6.35	5.97	5.97	4.40	53.83	23.49	7.27
Dargle at Dublin Road Bridge	3.07	3.23	27.69	1.29	21.41	43.31	60.12
Cookstown River at STP	14.18	10.69	8.96	7.05	50.84	8.28	24.05
Dargle at N11 Bridge	2.85	4.78	25.58	1.29	23.88	41.62	86.17
Kilmacanogue at N11 Bridge	4.19	19.66	8.68	6.05	30.03	31.39	8.74
County Brook (at Dargle)	11.95	11.78	17.38	2.07	48.30	8.52	5.51
Swan at Dargle	16.54	33.57	20.38	1.27	13.60	14.64	7.10
Harbour Mouth	4.37	8.57	23.08	1.68	25.49	36.81	114.15

Table 4.1: Water Level recorder sites (12)

Recorder Site	River	Type of Hydraulic Control for High Flows
Waterfall Bridge	Dargle	Channel
Onagh Bridge	Glencree	Channel
Dudley's Wood	Onagh Stream	Critical flow
Tumble Bay	Powerscourt Stream	Critical flow
Tinnahinch Bridge	Dargle	Channel
Boat Bridge	Killough	Channel
STP	Cookstown/Glencullen	Critical flow*
Dublin Road Bridge	Dargle	Critical flow
N11 Bridge	Dargle	Channel
Church	Kilmacanogue	Culvert entrance
Bray	County Brook	Pool
Bray	Swan River	Channel

**This was not obvious from a visual inspection, however it matched the flow gauging and modelling more closely than an equation based on uniform flow.*

Chapter 5

Spatial Precipitation inputs for TOPKAPI

5.1 Types of precipitation information available

In calibrating and testing the hydrological models, precipitation information is required. this may be from raingauges, or radar or some combination of the information from both sources.

Radar Surface Intensity Rainfall data are converted into rainfall accumulation data and then those are used with raingauge data to compute different adjustment factors. Different types of precipitation estimates are defined (e.g. raw radar or adjusted radar data).

5.2 Radar Adjustment factors

An adjustment factor is a constant by which a raw radar estimate of precipitation can be multiplied to obtain a corrected precipitation estimate. We distinguish between uniform and spatial adjustment factors. Please refer to Chapter **??** for an introduction to radar estimates correction techniques.

Uniform adjustment factors are the simplest adjustment technique. The mean radar bias is computed using all the raingauges and corresponding radar pixels data available in the catchment considered. The radar estimates can then be multiplied by the adjustment factor (also called correction factor). **?** applied the case to a 3500 km^2 catchment and

found a reduction in the mean error from 51% down to 35%.

When several raingauges data are available, an adjustment factor can be computed for each raingauge. The corrections of radar data are then carried out using the adjustment factor of the single closest raingauge to the radar estimate location. Errors have been shown to be smaller than by considering an average adjustment factor for the ensemble of raingauges available in the same area.

Six different methods of calculation of the adjustment factors are tested here. They are all based on the ratios of raingauge to radar measurements of precipitation G/R. In the following, $G_{i,T}$ denotes the precipitation accumulation during one time step at raingauge i at time T, and $R_{i,T}$ denotes the precipitation accumulation during one time step in the radar pixel corresponding to the location of raingauge i at time T, estimated from raw radar rainfall intensity data. n denotes the total number of time steps used in the analysis. N denotes the number of raingauges. Note that the denomination of the adjustment factors is subjective.

5.2.1 Uniform adjustment factor Type 1: A_{U1}

The spatial adjustment factor A_{U1} is defined as follows:

$$A_{U1} = \frac{1}{n} \sum_{T=1}^{T=n} \left[\frac{\sum_{i=1}^{i=N} G_{i,T}}{\sum_{i=1}^{i=N} R_{i,T}} \right] \tag{5.1}$$

where the summation is taken only over the time steps for which with $G_{i,T} > Min$ and $R_{i,T} > Min$ where Min is a minimum strictly positive, selected to avoid division by zero and the consideration of extreme fractions, when $R_{i,T} \ll G_{i,T}$. A minimum of 0.2 mm for a 1 hour accumulation is selected (**?**).

5.2.2 Uniform adjustment factor Type 2: A_{U2}

The spatial adjustment factor A_{U2} is defined as follows:

$$A_{U2} = \frac{1}{n} \sum_{T=1}^{T=n} \left[\frac{1}{N} \sum_{i=1}^{i=N} \frac{G_{i,T}}{R_{i,T}} \right] \tag{5.2}$$

with $G_{i,T} > Min$ and $R_{i,T} > Min$ where Min is a minimum strictly positive, selected to avoid division by zero and the consideration of extreme fractions, when $R_{i,T} \ll G_{i,T}$. A minimum of 0.2 mm for a 1 hour accumulation is selected (**?**).

5.2.3 Uniform adjustment factor Type 3: A_{U3}

The spatial adjustment factor A_{U3} is defined as follows:

$$A_{U3} = \frac{\sum_{T=1}^{T=n} \sum_{i=1}^{i=N} G_{i,T}}{\sum_{T=1}^{T=n} \sum_{i=1}^{i=N} R_{i,T}} \tag{5.3}$$

5.2.4 Spatial adjustment factor Type 1: A_{S1}

The spatial adjustment factor A_{S1} is defined as follows:

$$A_{S1} = \frac{1}{n} \sum_{T=1}^{T=n} \frac{G_{i,T}}{R_{i,T}} \tag{5.4}$$

with $G_{i,T} > Min$ and $R_{i,T} > Min$ where Min is a minimum strictly positive, selected to avoid division by zero and the consideration of extreme fractions, when $R_{i,T} \ll G_{i,T}$. A minimum of 0.2 mm for a 1 hour accumulation is selected (**?**).

5.2.5 Spatial adjustment factor Type 2: A_{S2}

The spatial adjustment factor A_{S2} is defined as follows:

$$A_{S2} = \frac{\sum_{T=1}^{T=n} G_{i,T}}{\sum_{T=1}^{T=n} R_{i,T}} \tag{5.5}$$

5.2.6 Spatial adjustment factor Type 3: A_{S3}

The spatial adjustment factor A_{S3} is defined as follows:

$$A_{S3} = \frac{\sum_{T=1}^{T=n} R_{i,T} G_{i,T}}{\sum_{T=1}^{T=n} R_{i,T}^2} \tag{5.6}$$

This is a new adjustment factor that minimises the sum of squares of the residuals between the raingauge and the radar data series. Thus, it tends to give more weight to the larger residuals which are usually associated with higher estimates of precipitation. However, this adjustment factor does not conserve the rainfall volumes, and should be used with caution. This adjustment factor is derived as follows:

At raingauge i, the sum of the squares of the residuals S can be written as:

$$S = \sum_{T=1}^{T=n} (G_{i,T} - \alpha R_{i,T})^2 \tag{5.7}$$

with α denoting the adjustment factor to be derived. Taking the derivative of S with respect to α:

$$\frac{dS}{d\alpha} = 2\alpha \sum_{T=1}^{T=n} R_{i,T}^2 - 2 \sum_{T=1}^{T=n} R_{i,T} G_{i,T} \tag{5.8}$$

Setting the derivative to zero, and solving for α, we obtain:

$$\alpha = \frac{\sum_{T=1}^{T=n} R_{i,T} G_{i,T}}{\sum_{T=1}^{T=n} R_{i,T}^2} = A_{S3} \tag{5.9}$$

To compute the adjustment factors, the radar and raingauge data at the same location for the entire calibration year 2002/2003 were considered. Adjustment factors were computed for different time steps: 15 minutes, 1 hour and 1 day, as shown on Tables 5.2, 5.3 and 5.4. Table 5.1 contains the yearly accumulations in mm for the raingauge and their corresponding radar pixels and it is clear that the raw radar data under-estimates the rain amounts measured by the raingauge.

In the following, 01,02,03,04 are the IDs for raingauges at Djouce, Powerscourt, Stone and Bray respectively. The number in brackets following the adjustment factor name in some cases is the minimum rainfall accumulation value selected for its computation.

Estimate	H0203				H0304			
	01	02	03	04	01	02	03	04
Raingauge	1580.3	1350.4	1422.6	1249.2	1272.1	1032.8	1190.0	828.6
Radar	518.9	518.0	439.5	555.9	382.0	372.8	363.9	341.9

Table 5.1: Yearly precipitation accumulations in mm.

Year 2002/2003 is noticeably wetter than year 2003/2004, as indicated by the yearly amounts for all the rainfall estimates on Table 5.1. This is due to extreme storms at the end of 2002, between November and December.

Although the Dublin weather radar was not functioning during a period of 3 weeks (August-early September) in 2003 and 2004, this has practically no effect on the values of the adjustment factors. The reason being that the period covering August and early September 2003 was exceptionally dry and that the corresponding period in 2004, although wetter, contributes only a small fraction of the annual rainfall.

The values obtained for year H0203 are very similar to the ones obtained for year H0304 for the 1 hour time step. It is therefore reasonable to assume adjustment factors constant in time, and to apply the adjustment factors determined from the calibration only to the radar data for the two years.

Adjustment factor A_{S3} is noticeably smaller than any other adjustment factor. This adjustment factor is new and minimises the errors between radar and raingauge estimates.

Adjustment factor	H0203			
	01	02	03	04
$A_{S1}(0.0)$	6.44	4.68	6.55	5.09
$A_{S1}(0.05)$	3.27	2.72	3.33	2.69
$A_{S1}(0.2)$	2.44	2.13	2.67	2.06
A_{S2}	3.05	2.61	3.24	2.25
A_{S3}	1.64	1.48	1.97	1.19
	Uniform			
$A_{U1}(0.0)$	7.84			
$A_{U1}(0.05)$	3.99			
$A_{U1}(0.2)$	2.77			
$A_{U2}(0.0)$	6.47			
$A_{U2}(0.05)$	2.99			
$A_{U2}(0.2)$	2.25			
A_{U3}	2.76			

Table 5.2: Adjustment factors for 15 minutes time step.

However, it does not account for volumetric correction, as the yearly corrected radar data accumulations do not match the yearly raingauge accumulations.

The minimum value selected, when required, influences the final estimate of the adjustment factor. A minimum of 0 mm is not acceptable. The value of 0.2 mm gives values that correspond to the other adjustment factors values.

Overall, most adjustment factors value are found to lie in the range [2.5-3.5] and those values are expected from the review of the literature on adjustment factors.

Adjustment factor	H0203				H0304			
	01	02	03	04	01	02	03	04
$A_{S1}(0.0)$	6.58	4.71	7.07	5.46	6.16	4.92	5.24	4.62
$A_{S1}(0.2)$	3.01	2.60	3.03	2.44	2.79	2.52	2.70	2.48
A_{S2}	3.05	2.61	3.24	2.25	3.32	2.77	3.26	2.42
A_{S3}	1.92	1.71	2.21	1.41	2.01	1.81	2.15	1.52
	Uniform				Uniform			
$A_{U1}(0.0)$	8.18				7.02			
$A_{U1}(0.2)$	3.38				3.23			
$A_{U1}(0.4)$	2.97				2.81			
$A_{U1}(0.8)$	2.66				2.53			
$A_{U2}(0.0)$	6.65				6.07			
$A_{U2}(0.2)$	2.78				2.68			
A_{U3}	2.76				2.96			

Table 5.3: Adjustment factors for 1 hour time step.

Adjustment factor	H0203			
	01	02	03	04
$A_{S1}(0.0)$	5.47	5.39	6.06	5.81
$A_{S1}(0.2)$	3.87	2.88	3.85	2.68
$A_{S1}(5.0)$	2.76	2.32	2.74	2.15
A_{S2}	3.05	2.61	3.24	2.25
A_{S3}	2.66	2.43	2.86	2.04
	Uniform			
$A_{U1}(0.0)$	5.75			
$A_{U1}(0.2)$	3.65			
$A_{U1}(20.0)$	2.44			
$A_{U2}(0.0)$	6.19			
$A_{U2}(0.2)$	3.37			
$A_{U2}(5.0)$	2.49			
A_{U3}	2.76			

Table 5.4: Adjustment factors for 1 day time step.

5.3 Processing to derive precipitation inputs

Different types of precipitation estimates were derived for the analysis. They include raingauge, raw radar and adjusted radar data. They are defined in Table 5.5 below. The data from those different types of precipitation are used subsequently for the analysis of the precipitation and as inputs into hydrological models for the analysis of flow rate estimates.

Adjustment factors A_{S2}, A_{S3} and A_{U3} were used to correct radar rainfall estimates. The other adjustment factors being very similar, no computation was required using them. Adjustment factors computed for a given time step were used to correct the precipitation accumulations for the same time step. In the following, "radar" means radar estimate at raingauge location, "all radar" means all the radar estimates over the specified area. Thiessen means the rainfall estimates are given for each Thiessen polygon over the catchment for use as input into a distributed or semi-distributed hydrological model. Otherwise, they are of uniform type and may be used as input into any type of hydrological model.

Type	Description	Spatial type
T1	raingauges	Thiessen
T2	radar	Thiessen
T31	radar adjusted A_{S2}	Thiessen
T32	radar adjusted A_{S3}	Thiessen
T4	average raingauges	uniform
T5	average radar	uniform
T61	average radar adjusted A_{S2}	uniform
T62	average radar adjusted A_{S3}	uniform
T7	average all radar over catchment area	uniform
T81	average all radar over catchment area adjusted A_{S2}	uniform
T82	average all radar over catchment area adjusted A_{S3}	uniform
T83	average all radar over catchment area A_{U3}	uniform
T9	average all radar over respective Thiessen area	Thiessen
T101	average all radar over respective Thiessen area adjusted A_{S2}	Thiessen
T102	average all radar over respective Thiessen area adjusted A_{S3}	Thiessen

Table 5.5: Types of precipitation estimates.

Chapter 6

Calibration of the models and simulation runs

The fitting/calibration of the lumped models to measured flow rate time-series and different combinations of precipitation input estimates, including raingauges, adjusted and raw radar data, is described in this section.

The two lumped models considered, namely the unit-hydrograph and SMARG are calibrated using the calibration year 2002/2003 (H0203) with hourly data for each type of rainfall estimate. A simulation using the parameters fitted for the calibration year is then produced to assess the calibration.

6.1 Unit-hydrograph model

The unit-hydrograph model was calibrated for a set of storm events selected in the year H0203 (see Table 6.1). The types of rainfall considered were: T4, T5, T61, T62, T7, T81, T82 and T83 and a unit-hydrograph was computed for each rainfall type (see Figure 6.1 and 6.2 for the calibration of the UH on the raingauge and the radar. The other radar UH are similar).

The direct runoff was estimated using a straight line between the beginning of the rise of the hydrograph and the start of the slow recession period. For each type of rainfall considered, effective rainfall was computed using two different methods: (1) constant fraction and (2) constant rate, so that the volume of effective rainfall equates the volume of the

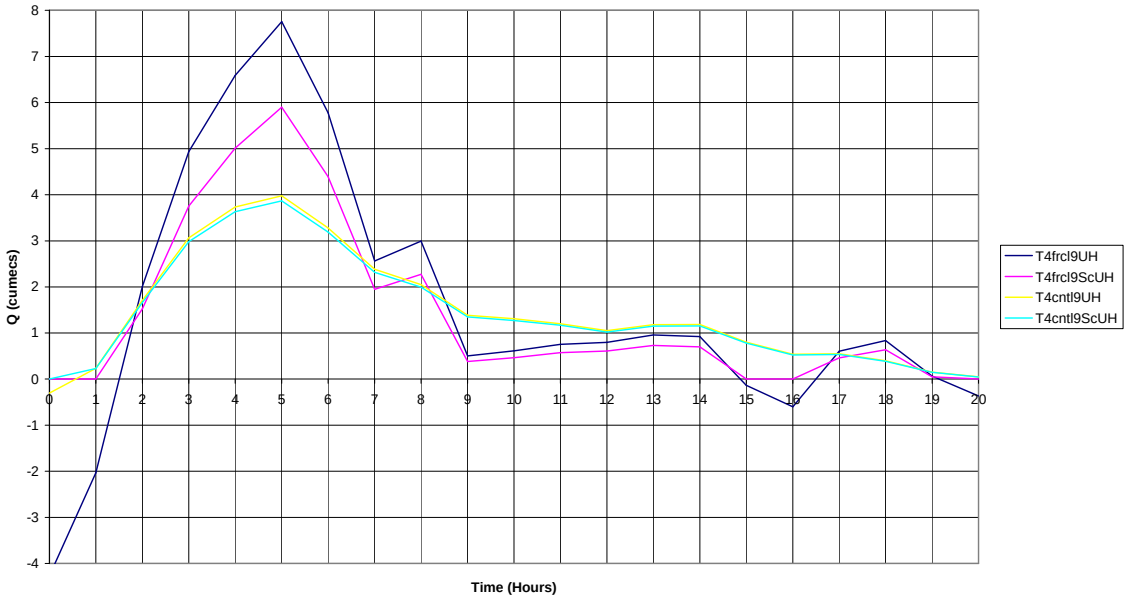

Figure 6.1: UH for Rain T4

direct runoff.

Fortran program "ker6tm" (Bruen and Dooge, 1984) was used to compute the unit-hydrograph ordinates with memory length of 20. No prior information was input and ridge regression was not applied.

The flow was then convoluted from the effective rainfall and the baseflow added for year H0203. For the validation year H0304, effective rainfall was derived using the loss function parameters in Table 6.2, which were derived for year H0203. The baseflow was removed using flow values derived for year H0203 (see Table 6.3). Refer to Figures 6.3, 6.4, 6.5, 6.6, 6.7, 6.8, 6.9, 6.10 for examples of results.

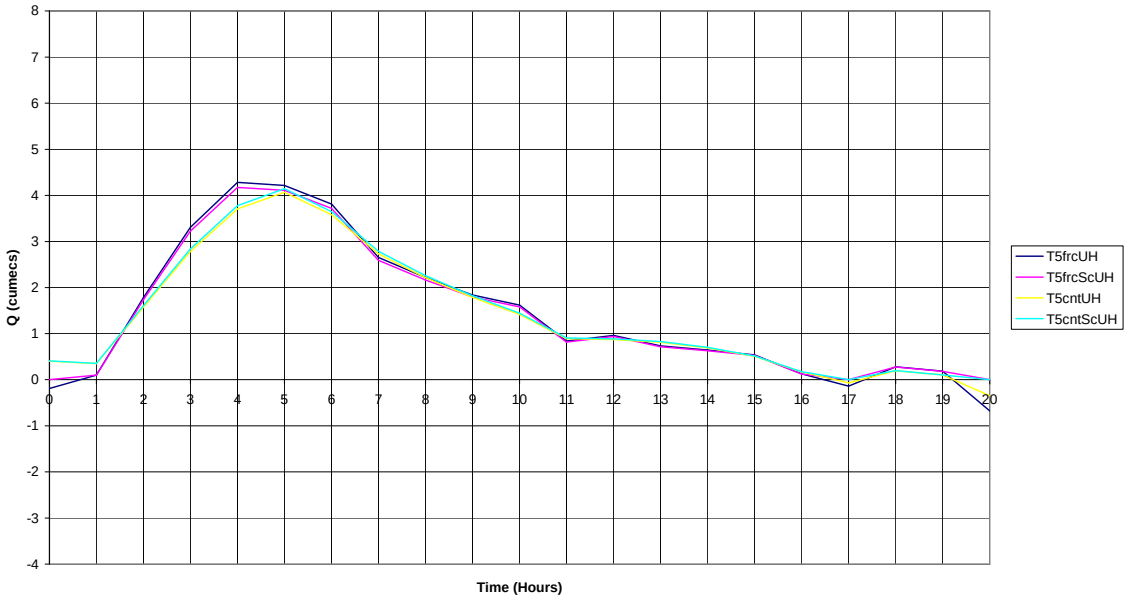

Figure 6.2: UH Rain T5

Year H0203		Year H0304	
Storm event ID	Period (days)	Storm event ID	Period (days)
St1	243-268	Stv1	498-561
St2	671-699	Stv2	708-745
St3	776-799	Stv3	992-1016
St4	1051-1107	Stv4	1045-1066
St5	1353-1419	Stv5	1417-1441
St6	1948-1974	Stv6	1484-1508
St7	2587-2608	Stv7	2552-2589
St8	2664-2687	Stv8	6375-6392
St9	3604-3662	Stv9	7729-7756
St10	4946-4969	Stv10	7768-7793
St11	5165-5198	Stv11	7831-7874
St12	5883-5912		
St13	6527-6548		

Table 6.1: Storm events used for the UH method.

Period and parameter	T4	T5	T61	T62	T7	T81	T82	T83
Summer frc	10.78	3.09	9.06	6.00	3.52	10.45	6.90	9.71
Summer cnt	3.55	0.61	3.28	1.81	0.76	3.81	2.20	3.44
Winter frc	5.39	1.75	5.05	3.33	1.90	5.60	3.72	5.23
Winter cnt	2.37	0.34	2.95	1.41	0.40	3.50	1.70	3.03

Table 6.2: Parameters of the loss functions.

Period in a year (days)	Baseflow (m^3/s)
1-1200	1.0
1200-3800	3.0
3800-end	3.0 down to 1.0 (line)

Table 6.3: Baseflow values.

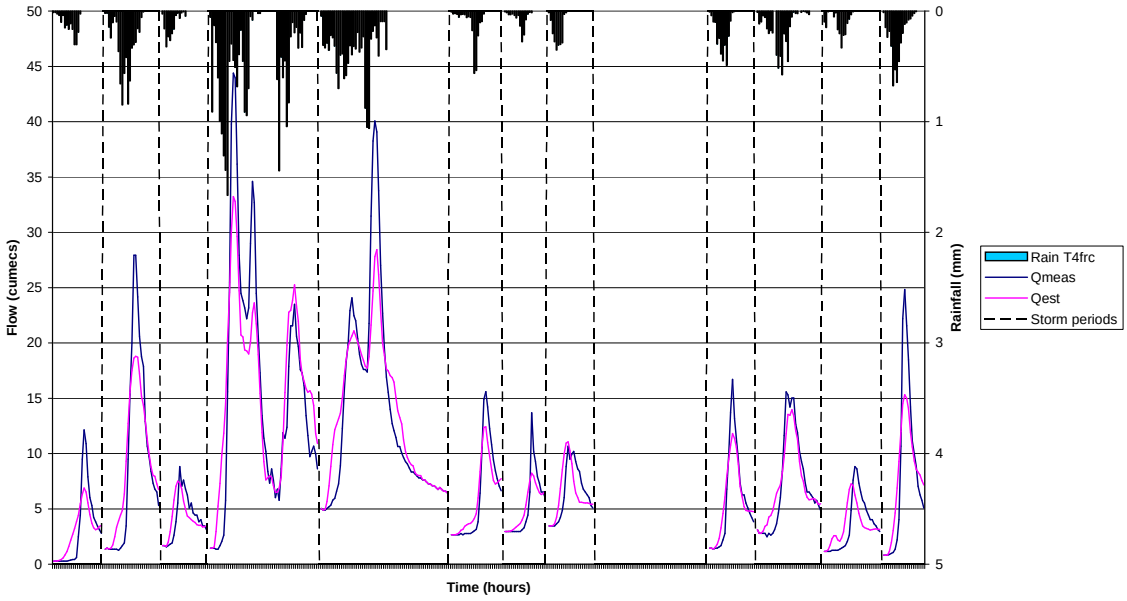

Figure 6.3: UH results for Rain T4frc over h0203

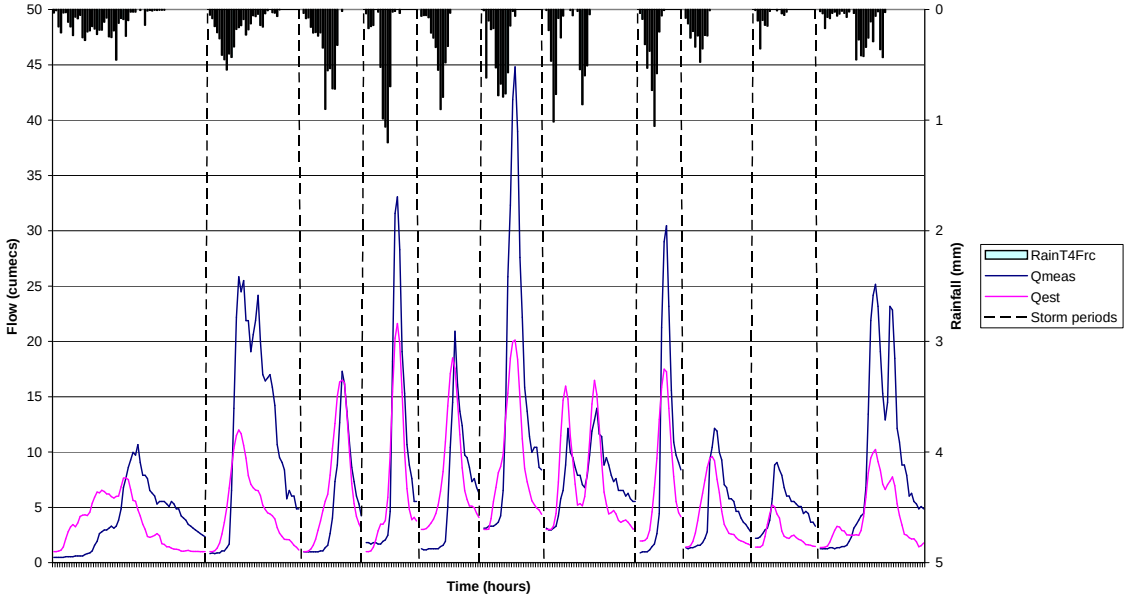

Figure 6.4: UH results for Rain T4frc over h0304

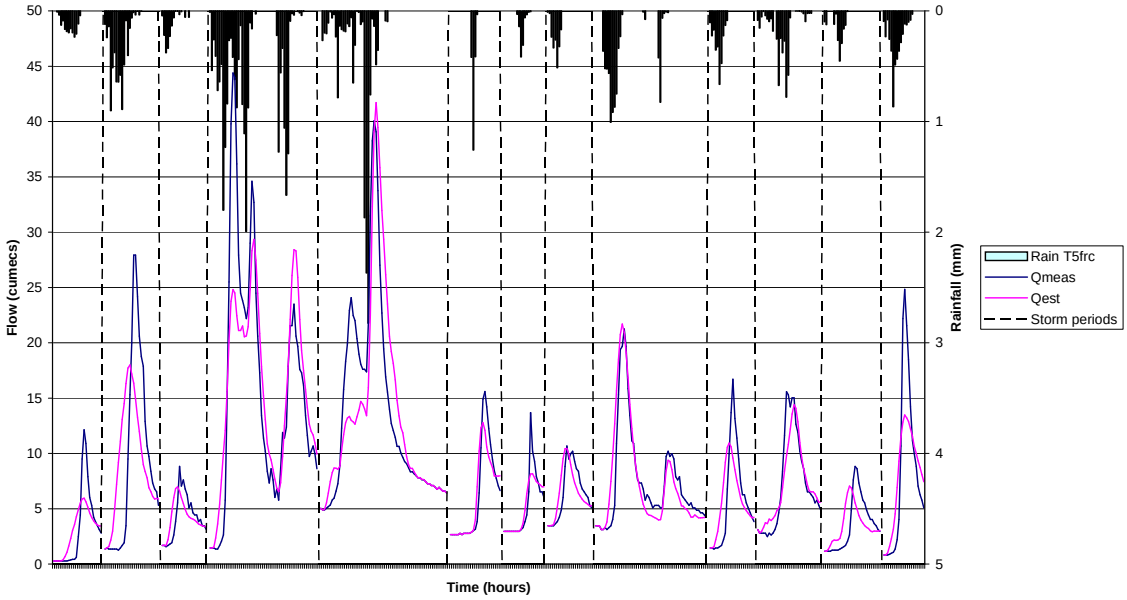

Figure 6.5: UH results for Rain T5frc over h0203

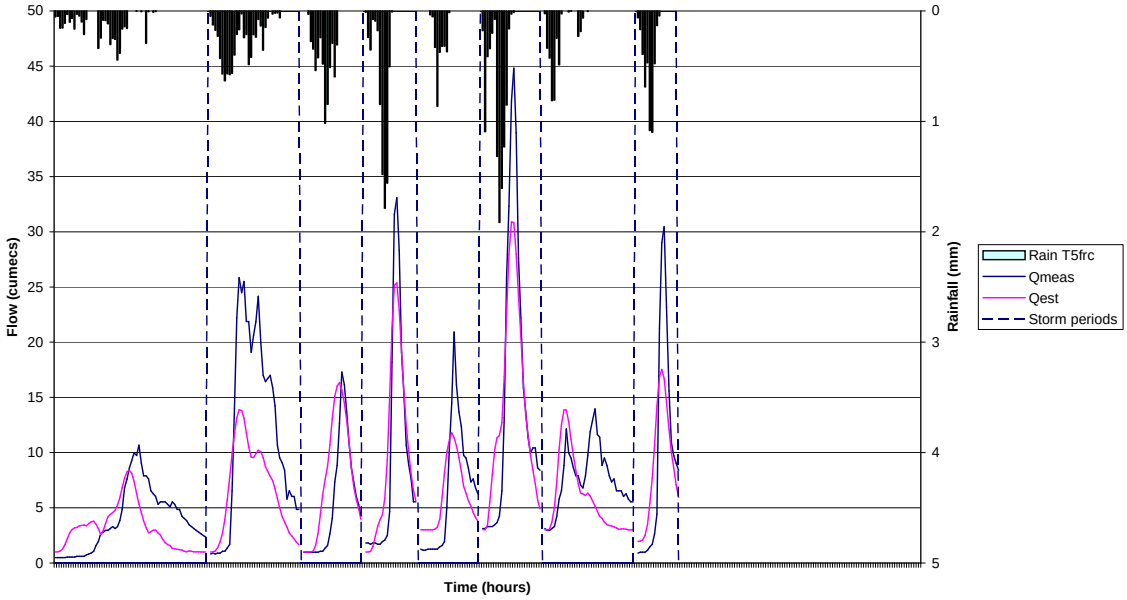

Figure 6.6: UH results for Rain T5frc over h0304

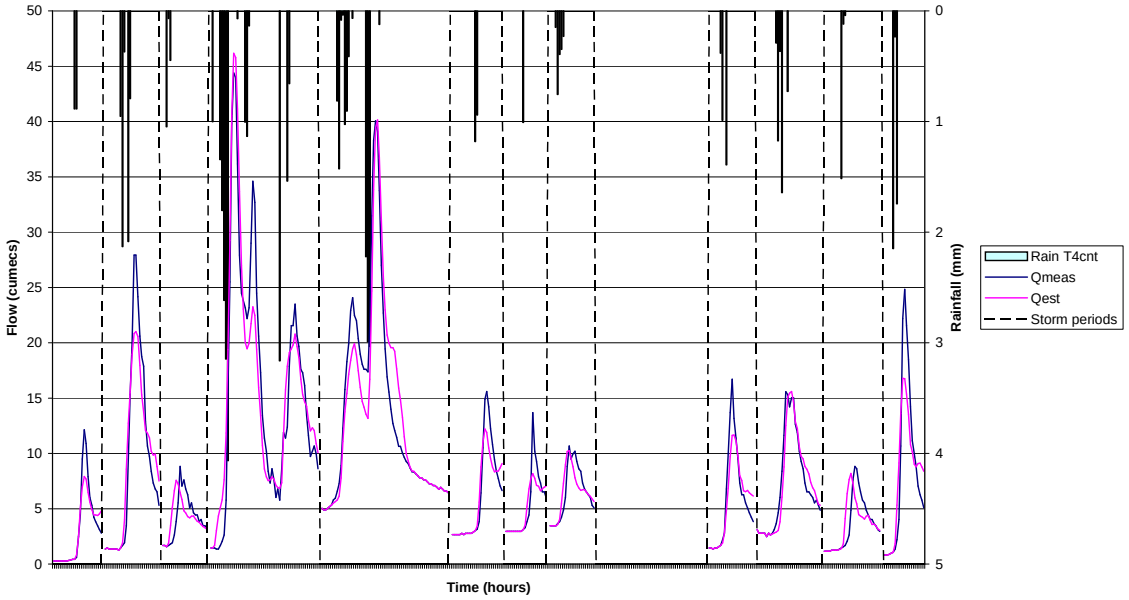

Figure 6.7: UH results for Rain T4cnt over h0203

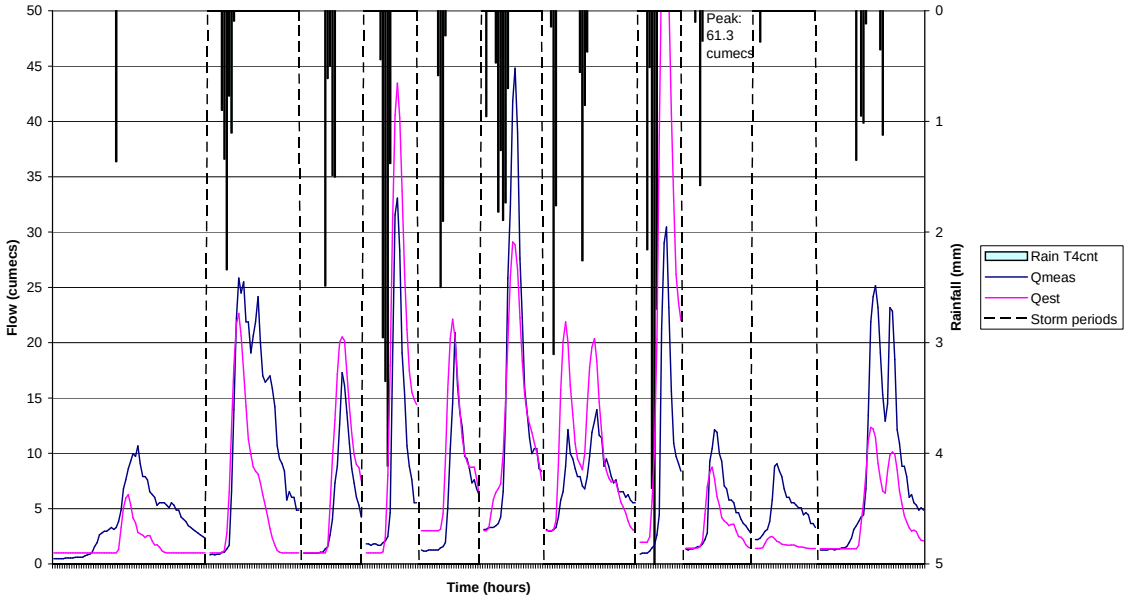

Figure 6.8: UH results for Rain T4cnt over h0304

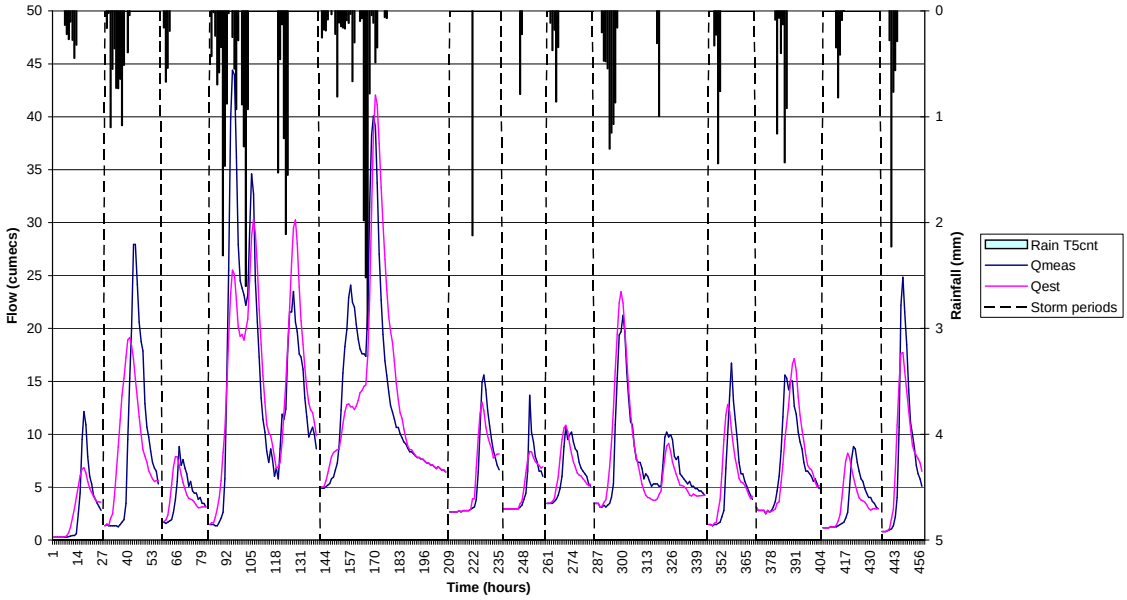

Figure 6.9: UH results for Rain T5cnt over h0203

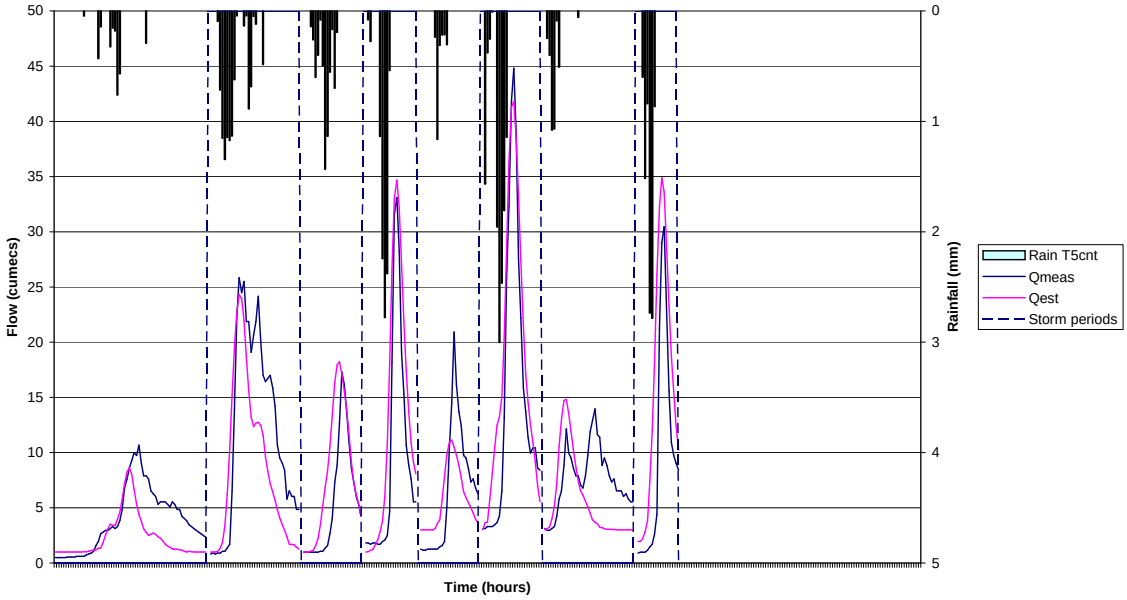

Figure 6.10: UH results for Rain T5cnt over h0304

6.2 SMARG model

The SMARG model was calibrated using evaporation, rainfall and flow rate data for year H0203. The model was calibrated for the uniform rainfall types: T4, T5, T61, T62, T7, T81, T82 and T83.

A specific objective function was fitted to the source code in order to optimise the simulated peak flow values. Peak were selected with a threshold of 15 m^3/s and at least two rising preceding ordinates and two decreasing subsequent ordinates.

Initial parameters values were selected from a previous run with the visual version of the model (see Table 6.4). The karstic parameter was set to 0 value. A unit-hydrograph memory length of 15 was chosen, as it is about 3 to 4 times the time to peak for the catchment considered. The fitted parameters for each input types are found in Table 6.4.

The simulation for the calibration and validation years were run with the same program, which can calibrate and simulate the flow for two subsequent periods.

Param.	Initial set up			Fitted parameters for each input type							
	Init.	Min	Max	T4	T5	T61	T62	T7	T81	T82	T83
T	0.557	0.5	1.0	0.99	0.50	0.99	0.88	0.57	0.82	0.68	0.82
H	0.031	0	1	0.004	0.76	0.10	0.44	0.79	0.00	0.00	0.00
Y	100	10	100	16.5	43.9	49.2	42.2	59.1	39.4	54.7	32.3
Z	102	25	125	114.3	114.3	25.0	25.0	113.3	25.1	124.9	25.1
C	0.92	0.50	1.00	0.79	0.72	0.89	0.75	0.78	0.76	0.99	0.71
F	0.0	0.0	0.0	0.0	0.0	0.0	0.0	0.0	0.0	0.0	0.0
G	0.81	0.0	1	0.65	0.04	0.74	0.76	0.0	0.75	0.75	0.73
N	1.79	1	10	1.03	2.62	1.83	1.92	1.00	1.00	1.00	1.00
NK	8.07	1	10	9.99	7.15	9.99	9.46	6.41	7.77	2.20	7.49
G	1384	1	6000	395	1.00	325	210	1083	421	304	378

Table 6.4: Initial and fitted SMARG parameters.

Chapter 7

Comparison of flow rates data from models simulations

An analysis is performed on the simulated discharges from the two lumped models considered. Charts and statistics are provided for the periods corresponding to the unit-hydrograph storm events only to compare SMARG, the unit-hydrograph method.

Dublin Airport weather radar was down due to maintenance operations: from 12 August 2003 to 2 September 2003 (in H0203) and from 14 August 2004 to 7 September 2004 (in H0304). The data for those periods are excluded from the analysis.

7.1 Comparison of SMARG and UH over the selected UH storms

Comparative statistics for the periods corresponding to the unit-hydrographs events are computed, taking the observed flow rates as the reference. frc and cnt refer to the fraction and constant loss functions. They only apply to the UH rainfall inputs. In year 2002/2003, storm 9 is exluded since the flow estimates are missing for the uh simulation with Rain T4frc and T4cnt. In year 2003/2004, storms v9, v10 and v11 are exluded, since the radar was not operating during the corresponding periods.

MSE, MRs and MAE statistics were computed for the continuous flow rate estimates series (see Tables 8.8, 8.9, 8.10).

MSE, MRs, ANPE and APTE statistics were calculated for the peaks only (see Tables 8.11, 8.12, 8.13, 8.14) for rain types T4 to T83 (uniform rainfall only). There were 8 peaks in the calibration year and 7 peaks in the validation year.

The unit-hydrograph outperforms the SMARG in calibration for the storm events. In calibration the case T4cnt is the best.

From the MRs statistics, it can be observed that the SMARG underestimates the flows for the non corrected radar only.

In terms of peak MSE, SMARG and UH are similar in calibration. There is a noticeable sensitivity to the loss function used.

However, the timing of peaks is best predicted by the UH. This is always true, except for T5, T61 and T62. There is no obvious improvement in calibration from using spatially variable correction factors.

Chapter 8

Conclusions

The unit-hydrograph and SMARG models were calibrated for a selection of precipitation estimates types. Two different loss function to derive the effective rainfall were used with the unit-hydrograph method.

Model outputs were compared over periods corresponding to the unit-hydrograph events. The unit-hydrograph method is sensitivity to the type of loss function used. The constant rate loss function can give peaks which are severely over estimated. Although the unit-hydrograph method generally gives better estimates for the timing of the peak, it does not out perform SMARG for the other statistics.

Type	Topkapi		SMARG	
	Cal.	Val.	Cal.	Val.
T1	8.70	5.32		
T2	7.03	4.47		
T31	10.91	6.68		
T32	5.10	3.93		
T4	8.84	5.28	6.07	3.48
T5	6.98	4.46	8.21	5.44
T61	10.78	6.65	7.32	4.68
T62	5.11	3.97	5.63	4.48
T7	6.75	4.50	8.91	5.87
T81	13.75	7.11	9.04	5.01
T82	5.18	4.12	6.81	4.87
T83	10.71	6.13	7.87	4.58
T9	6.73	4.49		
T101	14.07	7.22		
T102	5.15	4.09		
FD	11.48	6.23		

Table 8.1: MSE criterion for entire calibration and validation year for TOPKAPI and SMARG.

Type	Topkapi		SMARG	
	Cal.	Val.	Cal.	Val.
T1	2.14	1.48		
T2	-0.25	-0.01		
T31	2.06	1.63		
T32	0.83	0.75		
T4	2.13	1.46	1.24	0.49
T5	-0.23	-0.01	-1.33	-1.29
T61	2.05	1.59	1.23	0.74
T62	0.81	0.72	-0.32	-0.48
T7	-0.16	0.01	-1.30	-1.33
T81	2.36	1.72	1.85	1.12
T82	1.00	0.81	0.34	0.01
T83	2.09	1.54	1.53	0.88
T9	-0.16	0.02		
T101	2.39	1.78		
T102	1.03	0.85		
FD	2.03	1.48		

Table 8.2: MRs criterion for entire calibration and validation year for TOPKAPI and SMARG.

Type	Topkapi		SMARG	
	Cal.	Val.	Cal.	Val.
T1	2.23	1.73		
T2	1.29	1.14		
T31	2.26	1.87		
T32	1.48	1.31		
T4	2.23	1.71	1.51	1.06
T5	1.29	1.14	2.11	1.81
T61	2.25	1.85	1.58	1.27
T62	1.47	1.30	1.55	1.40
T7	1.28	1.14	2.13	1.84
T81	2.51	1.95	1.99	1.43
T82	1.55	1.35	1.35	1.20
T83	2.29	1.82	1.74	1.29
T9	1.28	1.14		
T101	2.54	1.99		
T102	1.56	1.36		
FD	2.24	1.78		

Table 8.3: MAE criterion for entire calibration and validation year for TOPKAPI and SMARG.

Type	Topkapi		SMARG	
	Cal.	Val.	Cal.	Val.
T1	55.57	92.15		
T2	415.91	467.73		
T31	120.70	34.17		
T32	132.68	184.96		
T4	55.02	84.89	39.98	83.27
T5	415.98	467.13	65.44	69.83
T61	120.83	33.10	39.36	49.56
T62	144.88	199.13	48.93	57.82
T7	400.94	478.27	81.98	104.02
T81	252.20	51.65	56.45	56.96
T82	118.20	220.03	74.73	52.14
T83	150.09	59.49	58.85	56.15
T9	397.74	476.77		
T101	267.59	47.06		
T102	108.03	205.67		
FD	305.5	97.78		

Table 8.4: MSE criterion for peaks over entire calibration and validation year for TOPKAPI and SMARG.

Type	Topkapi		SMARG	
	Cal.	Val.	Cal.	Val.
T1	2.19	-6.27		
T2	-18.79	-19.95		
T31	4.61	-1.38		
T32	-9.96	-12.67		
T4	2.46	-6.52	-1.80	-3.23
T5	-18.72	-19.92	-3.70	-6.85
T61	4.54	-1.66	-1.69	0.23
T62	-10.24	-13.06	-2.18	0.92
T7	-18.32	-20.01	-2.03	-8.37
T81	8.39	-1.83	-1.84	-3.30
T82	-8.44	-13.23	-0.41	-2.76
T83	4.36	-4.39	-1.95	-3.12
T9	-18.29	-19.99		
T101	8.81	-0.99		
T102	-7.97	-12.81		
FD	-8.15	-12.79		

Table 8.5: MRs criterion for peaks over entire calibration and validation year for TOPKAPI and SMARG.

Type	Topkapi		SMARG	
	Cal.	Val.	Cal.	Val.
T1	0.29	0.27		
T2	0.74	0.72		
T31	0.38	0.21		
T32	0.39	0.47		
T4	0.29	0.26	0.19	0.20
T5	0.73	0.72	0.25	0.24
T61	0.39	0.20	0.18	0.27
T62	0.39	0.48	0.21	0.32
T7	0.71	0.72	0.31	0.29
T81	0.50	0.22	0.21	0.18
T82	0.34	0.47	0.29	0.19
T83	0.41	0.23	0.22	0.18
T9	0.71	0.72		
T101	0.49	0.21		
T102	0.32	0.46		
FD	0.44	0.24		

Table 8.6: ANPE criterion for peaks over entire calibration and validation year for TOPKAPI and SMARG.

Type	Topkapi		SMARG	
	Cal.	Val.	Cal.	Val.
T1	1.36	2.43		
T2	1.64	1.14		
T31	2.36	2.00		
T32	2.07	1.86		
T4	1.57	2.43	1.29	2.14
T5	1.36	1.43	1.64	1.14
T61	2.50	2.29	2.07	0.86
T62	2.07	2.00	2.00	1.29
T7	1.43	1.29	2.21	2.14
T81	2.21	2.00	2.21	2.00
T82	1.71	2.00	2.57	2.71
T83	2.14	2.00	2.21	2.14
T9	1.57	1.14		
T101	2.00	2.00		
T102	1.64	1.86		
FD	2.21	2.00		

Table 8.7: APTE criterion for peaks over entire calibration and validation year for TOPKAPI and SMARG.

Type	Topkapi		SMARG		UH	
	Cal.	Val.	Cal.	Val.	Cal.	Val.
T4frc	36.57	39.00	35.64	47.71	8.97	33.38
T4cnt					5.73	55.39
T5frc	68.62	61.81	32.55	18.44	15.27	21.80
T5cnt					15.81	22.11
T61frc	48.33	47.78	34.93	43.29	15.19	21.55
T61cnt					26.47	121.87
T62frc	32.33	37.15	31.35	40.09	15.17	21.40
T62cnt					22.38	63.54
T7frc	66.29	63.43	43.79	35.80	17.78	28.92
T7cnt					20.25	26.35
T81frc	75.63	45.84	40.24	39.62	17.96	29.05
T81cnt					32.57	69.90
T82frc	30.66	38.61	54.60	65.52	17.92	29.13
T82cnt					28.85	45.87
T83frc	52.96	39.98	38.71	40.25	17.78	28.93
T83cnt					31.95	65.43

Table 8.8: MSE criterion for the unit-hydrograph events in calibration and validation year for TOPKAPI, SMARG and UH.

Type	Topkapi		SMARG		UH	
	Cal.	Val.	Cal.	Val.	Cal.	Val.
T4frc	3.61	1.46	4.23	3.61	-0.09	-1.77
T4cnt					-0.10	0.85
T5frc	-4.42	-3.32	-0.80	-0.80	-0.06	-1.12
T5cnt					-0.03	0.06
T61frc	2.58	1.97	3.35	4.36	-0.06	-1.06
T61cnt					-0.03	2.69
T62frc	-1.62	-1.15	1.53	3.35	-0.06	-1.05
T62cnt					-0.03	1.58
T7frc	-4.25	-3.31	-0.41	-1.26	-0.06	-1.66
T7cnt					-0.03	-1.15
T81frc	3.83	2.07	3.55	3.12	-0.06	-1.70
T81cnt					-0.03	-0.82
T82frc	-1.00	-1.09	0.56	0.74	-0.07	-1.69
T82cnt					-0.04	-0.91
T83frc	2.71	1.40	3.20	3.02	-0.06	-1.66
T83cnt					-0.03	-0.65

Table 8.9: MRs criterion for the unit-hydrograph events in calibration and validation year for TOPKAPI, SMARG and UH.

Type	Topkapi		SMARG		UH	
	Cal.	Val.	Cal.	Val.	Cal.	Val.
T4frc	4.31	4.75	4.85	4.94	1.88	4.17
T4cnt					1.51	4.57
T5frc	5.47	5.21	4.37	3.40	2.38	3.50
T5cnt					2.42	3.46
T61frc	4.54	4.95	4.57	5.21	2.38	3.48
T61cnt					3.03	6.90
T62frc	4.03	4.53	4.20	4.93	2.38	3.47
T62cnt					2.80	5.41
T7frc	5.35	5.24	4.80	4.59	2.55	3.58
T7cnt					2.58	3.75
T81frc	5.40	4.88	4.89	4.62	2.56	3.85
T81cnt					3.11	5.66
T82frc	3.88	4.54	5.08	5.84	2.56	3.87
T82cnt					2.93	4.80
T83frc	4.69	4.70	4.63	4.61	2.55	3.85
T83cnt					3.09	5.50

Table 8.10: MAE criterion for the unit-hydrograph events in calibration and validation year for TOPKAPI, SMARG and UH.

Type	Topkapi		SMARG		UH	
	Cal.	Val.	Cal.	Val.	Cal.	Val.
T4frc	22.71	84.89	48.58	83.27	64.58	185.97
T4cnt					31.41	229.40
T5frc	496.81	467.13	95.13	69.83	86.00	105.58
T5cnt					71.40	31.66
T61frc	147.65	33.10	60.74	49.56	58.84	101.47
T61cnt					125.73	412.59
T62frc	178.32	199.13	76.26	57.82	85.71	100.26
T62cnt					109.78	153.52
T7frc	485.34	478.27	120.84	104.02	107.10	168.49
T7cnt					104.65	84.40
T81frc	293.77	51.65	94.89	56.96	108.40	170.49
T81cnt					189.64	241.37
T82frc	159.20	220.03	120.70	52.14	106.44	168.58
T82cnt					166.13	134.89
T83frc	180.97	59.49	98.88	56.15	107.10	168.65
T83cnt					185.21	218.56

Table 8.11: MSE criterion for peaks for the unit-hydrograph events in calibration and validation year for TOPKAPI, SMARG and UH.

Type	Topkapi		SMARG		UH	
	Cal.	Val.	Cal.	Val.	Cal.	Val.
T4frc	2.52	-6.52	-2.09	-3.23	-7.00	-11.37
T4cnt					-3.77	1.12
T5frc	-20.45	-19.92	-4.83	-6.85	-6.81	-9.32
T5cnt					-5.58	-2.70
T61frc	4.96	-1.66	-3.00	0.23	-6.81	-9.06
T61cnt					-5.23	9.73
T62frc	-11.46	-13.06	-3.42	0.92	-6.80	-9.01
T62cnt					-5.10	4.33
T7frc	-20.03	-20.01	-2.87	-8.37	-7.48	-11.37
T7cnt					-6.08	-6.56
T81frc	8.83	-1.83	-2.79	-3.30	-7.52	-11.47
T81cnt					-5.19	-1.85
T82frc	-9.55	-13.23	-0.46	-2.76	-7.39	-11.39
T82cnt					-5.15	-3.10
T83frc	4.34	-4.39	-2.89	-3.12	-7.48	-11.38
T83cnt					-5.15	-1.49

Table 8.12: MRs criterion for peaks for the unit-hydrograph events in calibration and validation year for TOPKAPI, SMARG and UH.

Type	Topkapi		SMARG		UH	
	Cal.	Val.	Cal.	Val.	Cal.	Val.
T4frc	0.17	0.26	0.19	0.20	0.25	0.40
T4cnt					0.17	0.43
T5frc	0.75	0.72	0.27	0.24	0.26	0.35
T5cnt					0.23	0.20
T61frc	0.36	0.20	0.22	0.27	0.26	0.34
T61cnt					0.31	0.52
T62frc	0.41	0.48	0.25	0.32	0.26	0.34
T62cnt					0.29	0.36
T7frc	0.72	0.72	0.37	0.29	0.28	0.41
T7cnt					0.24	0.29
T81frc	0.55	0.22	0.30	0.18	0.28	0.42
T81cnt					0.33	0.57
T82frc	0.36	0.47	0.40	0.19	0.28	0.41
T82cnt					0.31	0.43
T83frc	0.45	0.23	0.31	0.18	0.28	0.41
T83cnt					0.32	0.53

Table 8.13: ANPE criterion for peaks for the unit-hydrograph events in calibration and validation year for TOPKAPI, SMARG and UH.

Type	Topkapi		SMARG		UH	
	Cal.	Val.	Cal.	Val.	Cal.	Val.
T4frc	1.38	2.43	1.25	2.14	0.75	1.43
T4cnt					1.00	1.57
T5frc	1.25	1.43	1.75	1.14	1.63	1.71
T5cnt					1.63	1.57
T61frc	2.50	2.29	2.38	0.86	1.63	1.57
T61cnt					1.75	2.00
T62frc	2.00	2.00	2.25	1.29	1.63	1.57
T62cnt					1.75	1.86
T7frc	1.38	1.29	2.25	2.14	1.75	1.14
T7cnt					1.63	1.71
T81frc	2.38	2.00	2.38	2.00	1.75	1.14
T81cnt					1.25	1.71
T82frc	1.88	2.00	2.63	2.71	1.75	1.14
T82cnt					1.00	2.00
T83frc	2.25	2.00	2.38	2.14	1.75	1.14
T83cnt					1.25	1.86

Table 8.14: APTE criterion for peaks for the unit-hydrograph events in calibration and validation year for TOPKAPI, SMARG and UH.

Bibliography

Bardsley, W. E. (1983). An alternative distribution for describing the instantaneous unit hydrograph. *Journal of Hydrology*, 62:375–378.

Barnes, B. S. (1959). Consistency in unit-hydrograph. In *Proc. ASCE(HY8)*, pages 39–63.

Bruen, M. and Dooge, J. C. I. (1984). An efficient and robust method for estimating unit-hydrograph ordinates. *Journal of Hydrology*, 70:1–24.

Clarke, R. T. (1994). *Statistical Modelling in Hydrology*. John Wiley and Sons.

Collins, W. T. (1939). Runoff distribution graphs for precipitation occurring in more than one time unit. *Civil Eng.*, 9(9):559–561.

Dooge, J. C. I. (1965). Analysis of linear systems by means of laguerre functions. *J. SIAM Control, Ser.A.*, 2(3):396–408.

Dooge, J. C. I. (1973). Linear theory of hydrologic systems. Technical report, U.S. Agricultural Research Service, Washington. Technical Bulletin No. 1468, 327pp.

Dooge, J. C. I. and Bruen, M. (1978). Linear algebra and unit-hydrograph stability. In *Int. Symp. Hydrology and Water Resources*, pages 157–179. Simon Bolivar University, Caracas, Venezuela.

Dooge, J. C. I. and Bruen, M. (1989). Unit-hydrograph stability and linear algebra. *Journal of Hydrology*, 111:377–390.

Dooge, J. C. I. and Garvey, B. J. (1978). The use of meixner functions in the identification of heavily damped linear systems. In *Proceedings of the Royal Irish Academy*, pages 157–179. Vol 78(A) No.18.

Draper, N. R. and Smith, H. (1998). *Applied regression analysis,* 3^{rd} *edition*. Wiley.

Duband, C., Obled, C., and Rodriguez, J. Y. (1993). Unit-hydrograph revisited: an alternative iterative approach to unit-hydrograph and effective rainfall identification. *Journal of Hydrology*, 150:115–149.

Eagleson, P. S., Mejia-R, R., and March, F. (1966). Computation of optimum realizable unit-hydrographs. *Water Resources Research*, 2(4):755–764.

Forsythe, G. and Moler, C. B. (1967). *Computer solution of linear algebraic systems*. Prentice-Hall.

Gouy, D. (1991). Comparaison de deux méthodes d'identification de la fonction de transfert et des pluies efficaces: application au bassin du gardon d'anduze. Mémoire de DEA, Un. Joseph Fourier, INPG, Grenoble, France.

Hoerl, A. E. and Kennard, R. W. (1970). Ridge regression, biaised estimation for non-orthogonal problems. *Technometrics*, 12(1):55–67.

Ivanov, V. K. (1963). O nekorrektno postavlennych zadachach. *Mat. sb.*, 63(2):211–223. (On ill posed problems, Mathematical proceedings 63) (in Russian).

Johnstone, D. and Cross, W. P. (1949). *Elements of Applied Hydrology*. N.Y. Ronald Press.

Kachroo, R. K. (1992). River flow forecasting. part 1. a discussion of principles. part 5. applications of a conceptual model. *Journal of Hydrology*, 133:1–15.

Khan, H. (1986). Conceptual modelling of rainfall-runoff systems. Master's thesis, National University of Ireland, Galway.

Kuchment, L. S. (1967). Solution of inverse flow problems for linear flow models. *Sov. Hydr. Pap.*, 2:194–199.

Lawson, C. L. and Hanson, R. J. (1974). *Solving least squares problems*. Prentice-Hall.

Liang, G. C. (1992). A note on the revised smar model. Workshop Memorandum, Dept. of Engineering Hydrology, National University College of Ireland, Galway (Unpublished).

Nash, J. E. (1958). The form of the instantaneous hydrograph. In *Gen. Ass. Toronto*, pages 3:114–118. IAHS Publ. No. 42.

O'Connell, P. E., Nash, J. E., and Farrell, J. P. (1970). River flow forecasting through conceptual models. part 2. the brosna catchment at ferbane. *Journal of Hydrology*, 10:317–329.

O'Connor, K. M. (1976). A discrete linear cascade for hydrology. *Journal of Hydrology*, 29:203–242.

O'Connor, K. M., Goswami, M., Liang, G. C., Kachroo, R. K., and Shamseldin, A. Y. (2001). The development of the galway real-time river flow forecasting system (gfmfs). In *The proceedings of the 19th European Regional Conference of ICID*.

O'Donnell, T. (1960). Unit-hydrograph derivation by harmonic analysis. *IAHS Publ.*, 51:546–557.

Sherman, L. K. (1932). Stream flow from rainfall by the unit-hydrograph method. *Engineering News Record*, 108:501–505.

Singh, V. P. (1988). *Hydrologic Systems, VolI: Rainfall-Runoff Modelling*. Prentice-Hall, N.J., USA.

Snyder, W. M. (1955). Hydrograph analysis by the method of least-squares. In *Journal of the Hydraulics Division, Proceedings of the American Society of Civil Engineers*, page 25. Vol. 81, No.793.

Tan, B. Q. and O'Connor, K. M. (1996). Application of an empirical equation in the smar conceptual model. *Journal of Hydrology*, 185:275–295.

Tan, B. Q., O'Connor, K. M., and Liu., Z. C. (1996). Application of a distributed form of the smar model. In *Proceedings: Volume 1, International Conference on Water Resources and Environment research: Towards the 21st Century. Water Resources Research Center, Kyoto University, Japan*.

Weisberg, S. (1980). *Applied linear regression*. Wiley.

Zhang, J. Y. (1992). Development of a user-friendly software system for the smar model. Master's thesis, National Univ. of Ireland, Galway.

Zhang, J. Y., O'Connor, K. M., and Liang, G. C. (1994). *A software package for river flow forecasting based on the SMAR model*, chapter in Water Resources and Distribution. Computational Mechanics Publications. Ed.: Blain, W.R. and Katsifarakis, K.L.